Article

A conserved flowering-time module underlies double-season cropping

https://doi.org/10.1038/s41586-026-11187-y

Received: 11 November 2025

Accepted: 18 September 2026

Published online: 04 November 2026

Check for updates

Guangqi Gao[1,2,7,11], Congcong Jiang[1,11], Wenxue Wu[1,11], Jinhong Kan[1], Yu Guo[2], Murukarthick Jayakodi[2,8], Chaodan An[1,9], Man Sun[1], Chunyuan Cheng[1,10], Jia-Wu Feng[2], Jianxia Wang[1], Jie Liu[1], Xia Li[1], Amanda Souza Camara[2], Xiao Xu[3], Hongyan Yang[3], Yawen Zeng[4], Huiquan Shen[3], Wenbin Zhou[1], Jing Zhang[1], Nils Stein[2,5], Martin Mascher[2,6] & Ping Yang[1]✉

Adapting crops to intensive cultivation systems under climate change requires varieties that combine yield potential with optimized flowering and maturation[1,2]. In central and eastern China, barley has long been cultivated in a double-season cropping system, in which early flowering and maturation are critical for escaping presummer terminal heat stress and enabling flexible rotation with summer crops[3,4]. Here we trace the genomic footprints of 80 years of modern breeding in China using 505 representative cultivars and identify a flowering-time module defined by a single amino acid substitution in PHYTOCHROME C in combination with a winter-type VERNALIZATION 1 haplotype that underpins this adaptation. The derived allele accelerates heading and maturity, and its frequency has risen sharply in modern autumn-sown varieties. Using base editing in barley and wheat, we confirm causality and demonstrate that this flowering-time combination module, *PhyC–VRN1*, is functionally conserved across Triticeae. Our results identify and experimentally validate a breeding-relevant flowering-time module that has been selected during modern breeding to enable intensive crop rotations, as well as demonstrate how precision genome editing can be used to reconstruct such adaptive modules for climate-resilient crop design.

Barley (*Hordeum vulgare* L.) and wheat (*Triticum aestivum* L.) are cornerstone cereals of global agriculture, valued for their versatility and ability to thrive across contrasting climates[1,5,6]. Their cultivation has expanded from Neolithic origins in the Fertile Crescent to high-latitude, arid and subtropical regions, reflecting the remarkable plasticity of flowering time in these species[2,7]. Natural variation in vernalization and photoperiod-response genes allowed farmers to fit cereals into local seasonal windows, enabling their spread from temperate origins into diverse environments[8,9]. Flowering time is modulated by an interplay of vernalization genes[10–13] and light responses[14–16], which together ensure reproductive success. These pathways are well studied, yet direct causal evidence linking specific haplotypes to large-scale agricultural adaptation remains rare. Identifying such haplotypes is especially important as cropping systems face increasing pressure from intensification and climate change[17].

China provides a compelling example of this challenge. Barley has been grown there for millennia[2], and has a striking role in the double-season cropping system in central and eastern parts of the country, where the crop is sown in autumn and harvested in late spring before sowing of summer crops (for example, rice). This rotation regime maximizes land use efficiency but requires rapid flowering and maturation to avoid presummer terminal heat stress and rainfall[3,4], as well as to ensure the timely sowing of summer crops. Since the mid-twentieth century, European malting barleys were introduced, bringing desirable yield and quality traits and prolonged life cycle[18]. Their successful integration in double-season rotations needed adaptation and genetic innovations in flowering behaviour that remain to be explained.

Previous studies pointed to a missense variant in the red/far-red light photoreceptor gene *PHYTOCHROME C* (*PhyC*) in barley that promotes flowering under long days[19,20]. Activated PhyC protein translocates from cytoplasm to the nucleus to suppress the *EARLY FLOWERING 3* (*ELF3*) centred evening complex, which functions as a direct transcriptional suppressor at the promoter region of the photoperiod-response gene *PHOTOPERIODIC 1* (*PPD1*)[21–23]. The phenylalanine-to-serine substitution at position 380 of PhyC was associated with early heading, but its causal role and agronomic importance were uncertain. Recent advances in base editing enable testing of such functional causality by precisely recreating natural single-nucleotide substitutions[24,25].

[1]State Key Laboratory of Crop Gene Resources and Breeding, Institute of Crop Sciences, Chinese Academy of Agricultural Sciences, Beijing, China. [2]Leibniz Institute of Plant Genetics and Crop Plant Research (IPK) Gatersleben, Seeland, Germany. [3]Institute of Agricultural Sciences of Coastal Area Jiangsu, Yancheng, China. [4]Biotechnology and Germplasm Resources Institute, Yunnan Academy of Agricultural Sciences, Kunming, China. [5]Crop Plant Genetics, Institute of Agricultural and Nutritional Sciences, Martin Luther University Halle-Wittenberg, Halle (Saale), Germany. [6]Centre for Crop and Food Innovation, Food Futures Institute, Murdoch University, Murdoch, Western Australia, Australia. [7]Present address: Leibniz Institute of Plant Genetics and Crop Plant Research (IPK) Gatersleben, Seeland, Germany. [8]Present address: Department of Soil and Crop Sciences, Texas A&M University, College Station, TX, USA. [9]Present address: Shiping County Government Offices Administration Bureau, Shiping, China. [10]Present address: College of Horticulture, Northwest A&F University, Yangling, China. [11]These authors contributed equally: Guangqi Gao, Congcong Jiang, Wenxue Wu. ✉e-mail: yangping@caas.cn

Although precision editing has transformed studies in model plants, applications in large-genome crops such as barley and wheat remain technically demanding. Demonstrating causality in these species would provide both a rigorous test of flowering-time hypotheses and a model for adaptation breeding.

Here we combine historical genomics[26,27], multi-environment field trials, genome-wide association mapping and functional validation to identify a breeding-relevant flowering-time module underlying adaptation to double-season cropping. We identify a single-nucleotide variant in *PhyC* that, in combination with a closely linked winter-type *vrn-H1*, defines a conserved flowering-time module that has been strongly enriched during modern breeding. Using base editing in both barley and wheat, we experimentally validate and demonstrate that this mechanism underpins adaptation to double-season cropping across Triticeae. These findings show how modern breeding has assembled and selected a conserved flowering-time module to fit cereals into intensive rotations, and demonstrate how precision genome editing can be used to reconstruct such adaptive modules for climate-resilient crop design.

Genomic footprints of breeding in China

To investigate how barley adapted to the double-season rotation systems in China, we assembled a panel of 532 cultivars spanning 80 years of breeding. This includes 505 popularly grown Chinese varieties, consisting of 186 in the 1940s–1950s (CN1940&50), 155 in the 1960s–1980s (CN60&70&80) and 164 in the 1990s–2010s (CN90&00&10), as well as 27 exotic lines that originated mostly from Europe and North America (Supplementary Table 1). This panel captured 82.39% of the cultivars included in the national barley variety directories published since the 1940s (refs. 26,27), representing the full diversity of row types, growth habits and end-use categories (Extended Data Fig. 1). Whole-genome resequencing generated roughly 18 terabases of clean sequence, yielding an average depth of roughly 8 times per cultivar and identifying more than 23 million high-quality single-nucleotide polymorphisms (SNPs) (Supplementary Tables 2 and 3). Population structure analysis revealed three separate groups: historic Chinese cultivars with predominantly East Asian ancestry; Tibetan qingke (six-rowed naked barley), which retained Central Asian ancestry[28], and modern Chinese cultivars, which carried large European genomic contributions (Fig. 1a). When projected onto global panels of cultivated barley[29,30], historic Chinese varieties clustered with East Asian landraces, whereas modern cultivars clustered closer to European germplasm (Fig. 1a,b). The highest nucleotide diversity was observed in cultivars from the period of the 1960s–1980s, when exotic lines were most widely introduced, and the diversity declined thereafter due to directional selection for agronomic performance (Fig. 1c). Genetic differentiation analysis revealed a lower differentiation index (F_{st}) between Chinese modern cultivars and exotic lines (F_{st} = 0.0655), both showing greater differentiation from CN1940&50, whereas qingke represented higher divergence to all other groups. Genome-wide diversity in qingke has not undergone a continuous erosion; instead, shifts in ancestry composition driven by the loss and subsequent reintroduction of specific haplotypes during breeding were observed (Supplementary Fig. 1). Germplasm identity-by-descent (gIBD) networks highlighted five main pedigree groups in Chinese cultivars, reflecting the predominant contributions of a small number of foundation lines in the breeding history (Extended Data Fig. 2a,b and Supplementary Table 4). Modern cultivars showed complex mosaics of ancestry, indicating recurrences of recombination and selection (Extended Data Fig. 2c). These results demonstrate a profound shift in the genomic composition of Chinese barley during the twentieth century. East Asian haplotypes were progressively replaced by European haplotypes over decades, enriching genetic diversity and enabling the development of high-yielding malting and feed varieties. At the same time, the regional specialized breeding of Tibetan qingke maintained its distinct Central Asian genomic framework (Fig. 1b), despite evidence of limited gene flow (Extended Data Fig. 2a).

These genomic changes were accompanied by striking trends of phenotypic alterations observed in multi-location field trials across three representative agroecological environments (Supplementary Figs. 2–4). Field trials under common modern cultivation systems revealed that, historic cultivars headed later, matured more slowly and were taller in plant height, making them poorly adapted to double-season rotations (Fig. 1d and Extended Data Fig. 3a,b). By contrast, modern cultivars flowered and matured earlier, presented shorter in stature and produced heavier grains. Quantitatively, plant height declined by about 20% on average, whereas grain width and thousand-grain weight both increased significantly. Across two growing seasons and three locations, modern cultivars consistently outperformed exotic lines in earliness, aligning with the agronomic need to harvest barley before the onset of terminal heat stress and rainfall (Extended Data Fig. 3a).

Genome-wide association mapping for ten agronomic traits confirmed the broad genetic basis of these changes, with expected signals at loci such as *NUD* (hull adherence[31]), *Vrs1* (row type[32]) and *uzu/HvBRI1* (plant stature[33]) (Extended Data Fig. 4 and Supplementary Table 5). Among 25 pleiotropic loci, a major signal on the long arm of chromosome 5H stood out, influencing heading date, maturity date, plant height and yield components (Fig. 2a and Extended Data Fig. 4). This locus, harbouring both flowering regulatory genes *PhyC* and *VERNALIZATION 1* (*VRN-H1*), became the focus of further investigation.

A flowering-time variant in *PhyC*

We first examined sequence variations in *PhyC* and *VRN-H1* across the 532 cultivars. *VRN-H1* encodes a MADS-box transcription factor required for the transition to reproduction phase[10,11]. *VRN-H1* haplotypes are defined by length polymorphisms in the first intron[34]. The ancestral winter-type *vrn-H1* allele retains an intact intron 1 of roughly 11 kilobases (kb). Cold treatment (vernalization) upregulates *VRN-H1* expression, thereby promoting flowering. By contrast, spring-type *Vrn-H1* alleles carry deletions of various length on the first intron and confer dominant inheritance of flowering independent of vernalization. We identified ten *VRN-H1* haplotypes, including a new variant V1-11 (Extended Data Fig. 5 and Supplementary Table 1). In autumn-sown field trials, the two alleles did not show a difference on heading date (Fig. 2b). Sequence analysis defined 16 haplotypes of *PhyC* (Supplementary Table 6). Two haplotypes (Hap15 and Hap16) shared a single T-to-C substitution at coding DNA sequence position 1139, introducing a phenylalanine-to-serine substitution (F380S) in the conserved GAF domain. These derived haplotypes (1139C) strongly associated with earlier heading (Fig. 2b) and were designated *PhyC-e* (early flowering), whereas all others (1139T) were classified as *PhyC-l* (late flowering). This indicates *PhyC* as the likely causal gene for the heading date association peak on 5H. The *PhyC-e* allele was found in 111 Chinese cultivars and an exotic Japanese variety, but absent from European or other geographically diversified lines, suggesting an East Asian origin (Supplementary Table 1). Screening in global diversity panels of 2,231 accessions including wild and cultivated barley further confirmed its specificity (Supplementary Table 7). Haplotype network analysis and GEVA-based dating were consistent with a relatively recent origin of *PhyC-e* from the ancestral haplotype Hap01 (Fig. 2c, Supplementary Fig. 5 and Supplementary Table 8), and the *PhyC-e* haplotype was restricted to East Asian landraces and modern cultivars (Fig. 2d).

To further validate its effect under homogeneous genetic backgrounds, we developed near-isogenic lines (NILs) targeting the *PhyC* genotypic segregation on the background of spring-type *Vrn-H1* (NIL-set1; Extended Data Fig. 6a–c). The *PhyC-e* confers earlier heading and maturity under autumn-sown conditions (Extended Data Fig. 7a,c), or early-February sown conditions (in Beijing where vernalization requirements are met but the vegetative growth phase is shortened,

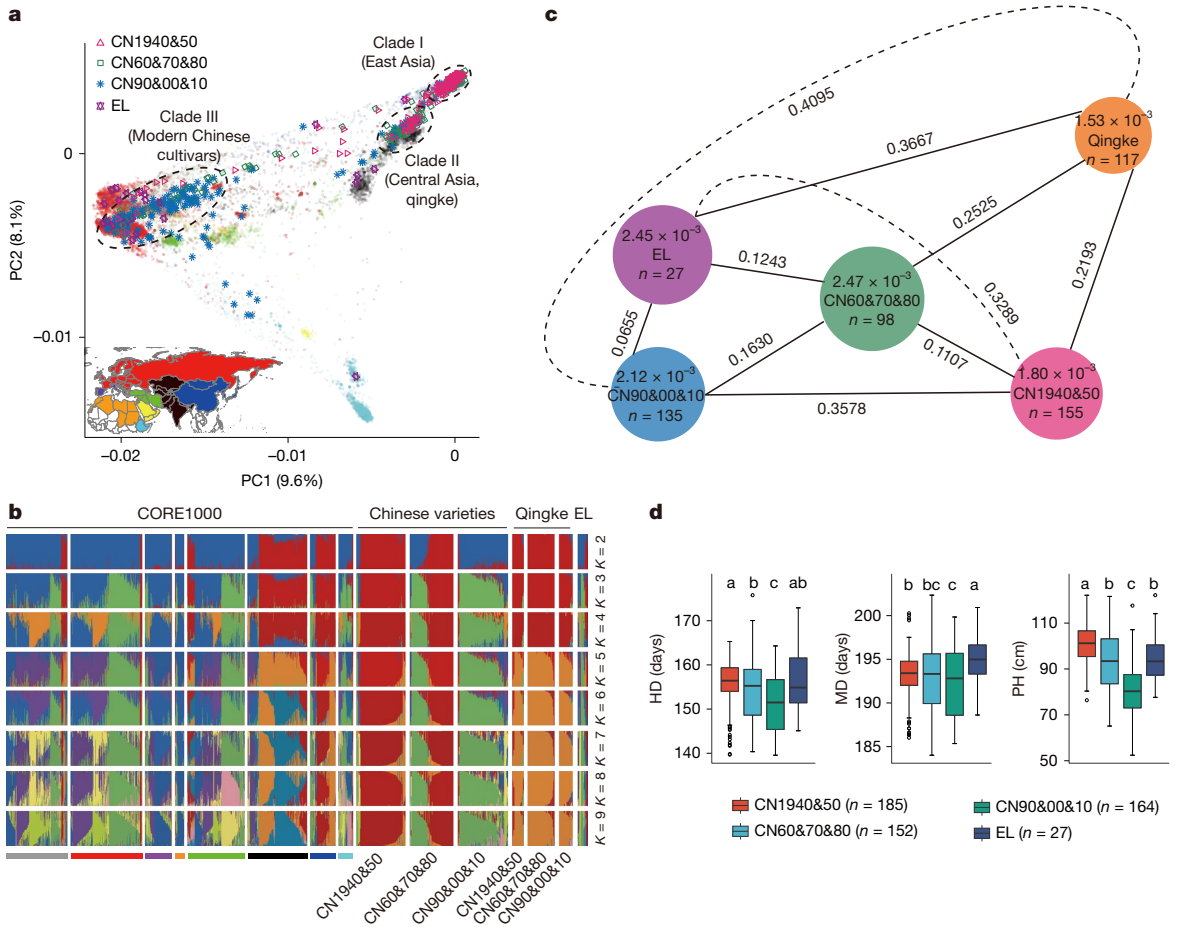


Fig. 1 | Genomic and phenotypic diversity of Chinese barley cultivars across eight decades. a, Nucleotide variation-based principal component analysis of the 532 varieties compared with 19,778 globally diverse cultivated barley accessions from genebanks[29]. Background colours represent geographically regional groups based on passport data, and foreground shapes denote chronologically grouped Chinese varieties. Percentages on the axes indicate variance explained by PC1 and PC2. **b**, ADMIXTURE ancestry coefficients for *K* ranging from 2 to 9 for a total of 1,532 accessions, including the global representative barley collection CORE1000 (ref. 30) and the 532 varieties analysed in this study. The coloured blocks below the CORE1000 bar plots correspond to the regional grouping in **a**. The grey block corresponds to North American origin. Qingke barleys were separately grouped beside 388 other Chinese varieties. **c**, Nucleotide diversity (π, within cycles) and population divergence (F_{st}, on lines) among five groups including the distinctive qingke barley as an independent group. **d**, Heading date (HD), maturity date (MD) and plant height (PH) of Chinese barley cultivars. The box plots are generated according to BLUE values across several trials. Box plots show the 25–75% interval of raw value in the box, with central lines indicating the median and whiskers extending to the minimum and maximum values within 1.5× of the interquartile range; outliers beyond this range are shown as individual circles. Different letters indicate significant differences at $P \leq 0.05$, determined by one-way ANOVA followed by Fisher's least significant difference test. EL, exotic lines; PC, principal component.

thereby increasing vulnerability to terminal heat stress) (Extended Data Fig. 7b), explaining its value in double-season cropping systems in which heat escape is crucial. These findings suggest that a single missense mutation in *PhyC* has played a central role in the adaptation of Chinese barley to intensive double-cropping. However, early-flowering plants carrying *PhyC-e* were detected with reduced biomass and yield components (Extended Data Fig. 7d,e), traits that are undesirable from a breeding perspective.

Interaction with winter-type *vrn-H1*

PhyC-e promotes early flowering but carries potential fitness costs, pointing towards the importance of its linked haplotype combinations in breeding history. As *PhyC* lies only around 369 kb from *VRN-H1*, we asked whether their haplotype combination might be selected as a module for the success of early-flowering barley in China. Three combinations of *PhyC* and *VRN-H1* alleles were identified in the 2,231 sequenced barley accessions: *PhyC-l* + *Vrn-H1* (spring-type late-flowering module); *PhyC-l* + *vrn-H1* (winter-type late-flowering module) and *PhyC-e* + *vrn-H1* (winter-type early-flowering module) (Fig. 3a and Supplementary Table 7). Cross-population composite likelihood ratio test (XP-CLR) scans, nucleotide diversity (π) and haplotype-based selection analysis were consistent with a roughly 4.6 Mb selective sweep encompassing both genes and present only in accessions carrying the *PhyC-e* + *vrn-H1* module (Supplementary Figs. 6 and 7). Across 341 wild barleys and 1,328 exotic lines, two modules *PhyC-l* + *Vrn-H1* and *PhyC-l* + *vrn-H1* were predominant (Fig. 3b). Historic autumn-sown Chinese cultivars were dominated by the *PhyC-l* + *vrn-H1* module. From the 1960s onwards, however, this module was progressively displaced by *PhyC-e* + *vrn-H1*, which has accounted for more than 60% of autumn-sown modern varieties since the 1990s (Fig. 3b,c). By contrast, spring-sown cultivars in northern China (one season annually) remained largely fixed with the *PhyC-l* + *Vrn-H1* module (Fig. 3b). These shifts mirror the divergent agronomic requirements of the two cropping systems. Field phenotyping confirmed that the *PhyC-e* + *vrn-H1* module provided the optimal balance of agronomic traits under double-season cropping conditions. This haplotype module enabled earlier flowering and maturity while maintaining yield-related components

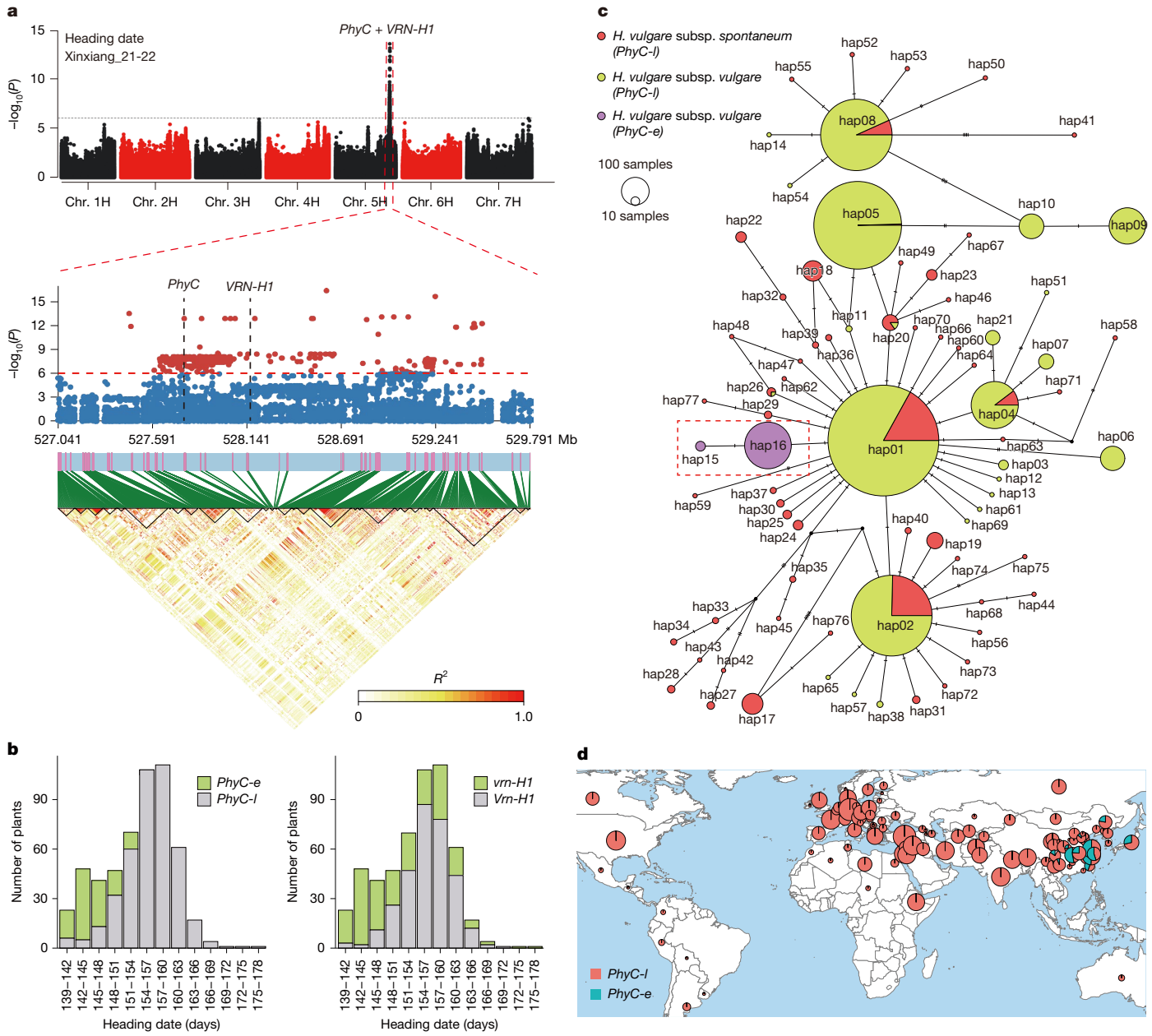


Fig. 2 | The *PhyC-e* variant promotes early heading. a, The most significant association to the heading date variation was detected on chromosome 5H from the trial 'Xinxiang_20-21'. The known flowering-time regulatory genes *PhyC* and *VRN-H1* are located within the association interval. The lower panel shows association peaks within the 2.75 Mb physical interval. The local linkage disequilibrium estimation identified *PhyC* and *VRN-H1* in separate linkage disequilibrium blocks. Marker–trait associations were tested using a mixed linear model, with multiple-testing correction performed using the Benjamini–Hochberg procedure. Associations with significance at $P < 1 \times 10^{-6}$, corresponding to a false discovery rate of 0.05, were considered. **b**, *PhyC* and *VRN-H1* haplotypes distribution in discrete groups of varieties with varied heading date. **c**, Median-joining networks for the *PhyC* nucleotide haplotypes among the 2,231 barley accessions, including the wild barley collection WBDC[37] and WILD100 (ref. 30), the domesticated barley collection CORE1000 (ref. 30), the European elite variety collection SHAPE_cv315 (ref. 30) and the 532 varieties analysed in this study. **d**, Global distribution of the *PhyC-e* and *PhyC-I* haplotypes among 2,231 barley accessions. LD, linkage disequilibrium. Geographical outlines in **d** were reproduced from the maps R package (https://CRAN.R-project.org/package=maps), which uses public domain base-map data (under a GNU General public license, version 2).

under field conditions (Fig. 3d), thereby offsetting the drawbacks of *PhyC-e* when present at the spring-type *Vrn-H1* background (Extended Data Fig. 7d,e).

To validate these observations, we developed NILs (NIL-set2) segregating at *PhyC* on the background of winter-type *vrn-H1* (Extended Data Fig. 6a–c). In field trials in Beijing under early-spring-sown conditions facing terminal heat stress (Extended Data Fig. 7b), NILs carrying the *PhyC-e* + *vrn-H1* module consistently flowered and matured earlier, with higher harvest index and improved grain weight (Fig. 4a). However, in the greenhouse with optimal growth conditions that is free of heat stress, the early-heading lines showed reduced biomass and yield if compared with the late-heading lines (Fig. 4b). These results demonstrate that the advantage of *PhyC-e* + *vrn-H1* module is context dependent and highly beneficial in double-season cropping. Transcript profiling supported this interpretation. Plants carrying *PhyC-e* showed elevated expression of downstream flowering regulatory genes including *PPD-H1*, *FT1* and *VRN-H1*, specifically under long-day conditions (Fig. 4c). *PhyC* transcript levels themselves were unchanged between

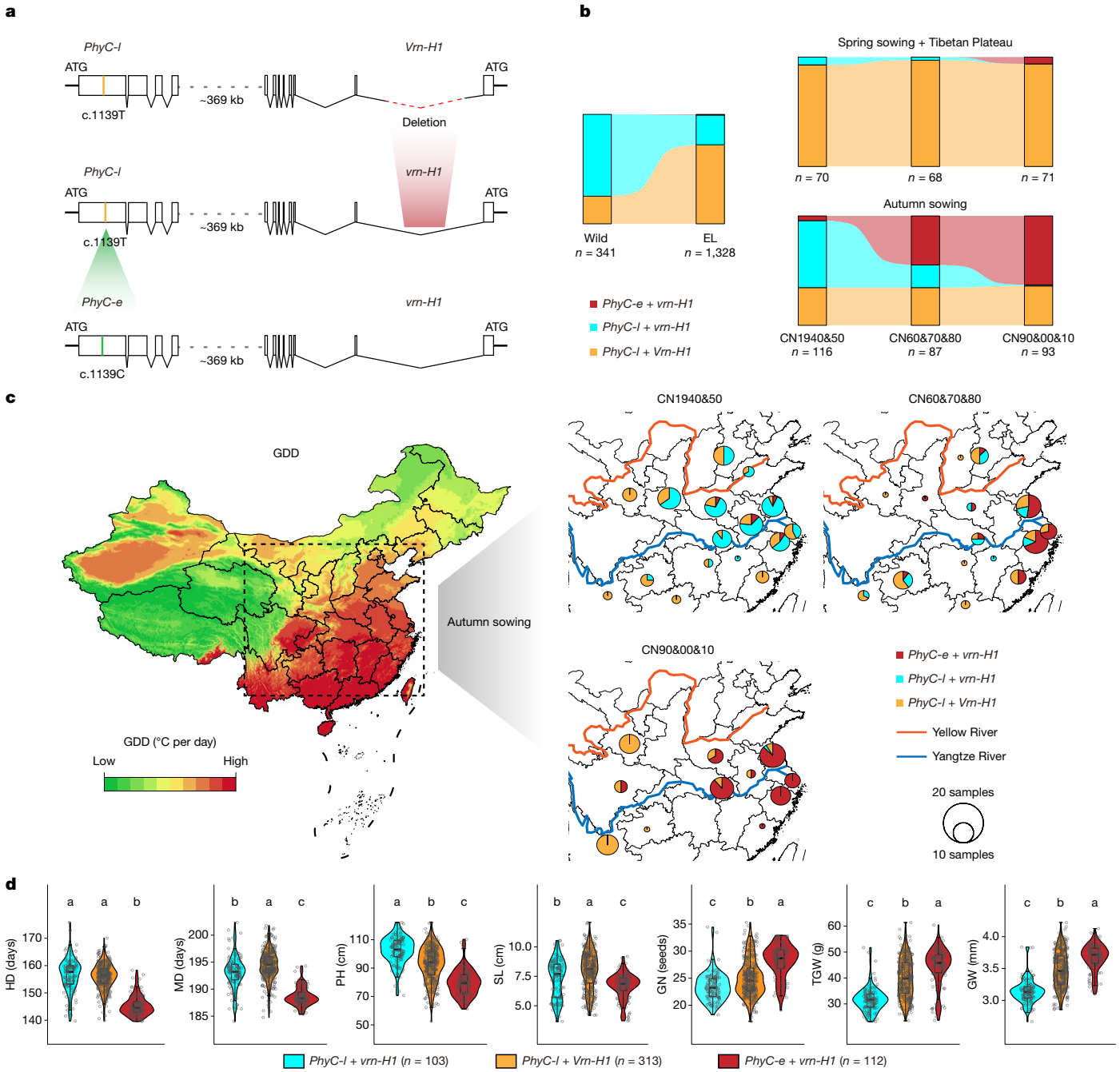


Fig. 3 | Selection of *PhyC-e* and *VRN-H1* haplotype combination. a, Three haplotype combinations at the *PhyC* and *VRN-H1* locus identified from 532 cultivars. **b**, Frequency of haplotype combinations in wild barley, exotic lines and Chinese barley cultivars (CN). Wild barley comprises 255 accessions from the WBDC panel[37] and 86 accessions from the WILD100 panel[30], whereas exotic lines includes 27 accessions from this study and another 1,301 landraces and/or cultivars from a barley pangenome study[30]. **c**, Frequency of haplotype combinations in cultivars categorized by ecological zones. The left panel shows nationwide divergence of the growing degree days (GDD) during 1970–2020, whereas the areas indicated by the dashed box normally have barley grown in autumn-sowing mode. The three sections on the right side show gradual enrichment of the *PhyC-e* + *vrn-H1* combination along the middle and downstream of the Yangtze River valley. Geographical boundaries of China, including provincial boundaries and the dashed line, were reproduced from the China-GeoData dataset (https://github.com/Supeset/China-GeoData) under an MIT license. **d**, BLUE statistics of seven adaptation-related phenotypic traits among different *PhyC* and *VRN-H1* combinations. In violin plots, the width represents the enrichment of raw values. The central line in each box indicates the median, the box represents a 25–75% interval of the raw values and the whiskers extend to the minimum and maximum values within 1.5× of the interquartile range. Different letters indicate significant differences at $P \leq 0.05$, determined by one-way ANOVA followed by Fisher's least significant difference test. GN, grain number on two rows per spike (two central spikelets of six rows are counted in six-rowed barley); GW, grain width; SL, spike length; TGW, thousand-grain weight.

haplotypes, suggesting that the missense variant alters protein function rather than gene expression. The accelerated transition to flowering enabled this barley genotype to be ready for harvest earlier in the season, which avoids heat stress. The NILs also showed pleiotropic effects of *PhyC* on plant architecture and spike morphology (Fig. 4a), aligning with the patterns observed in modern cultivars (Fig. 3d).

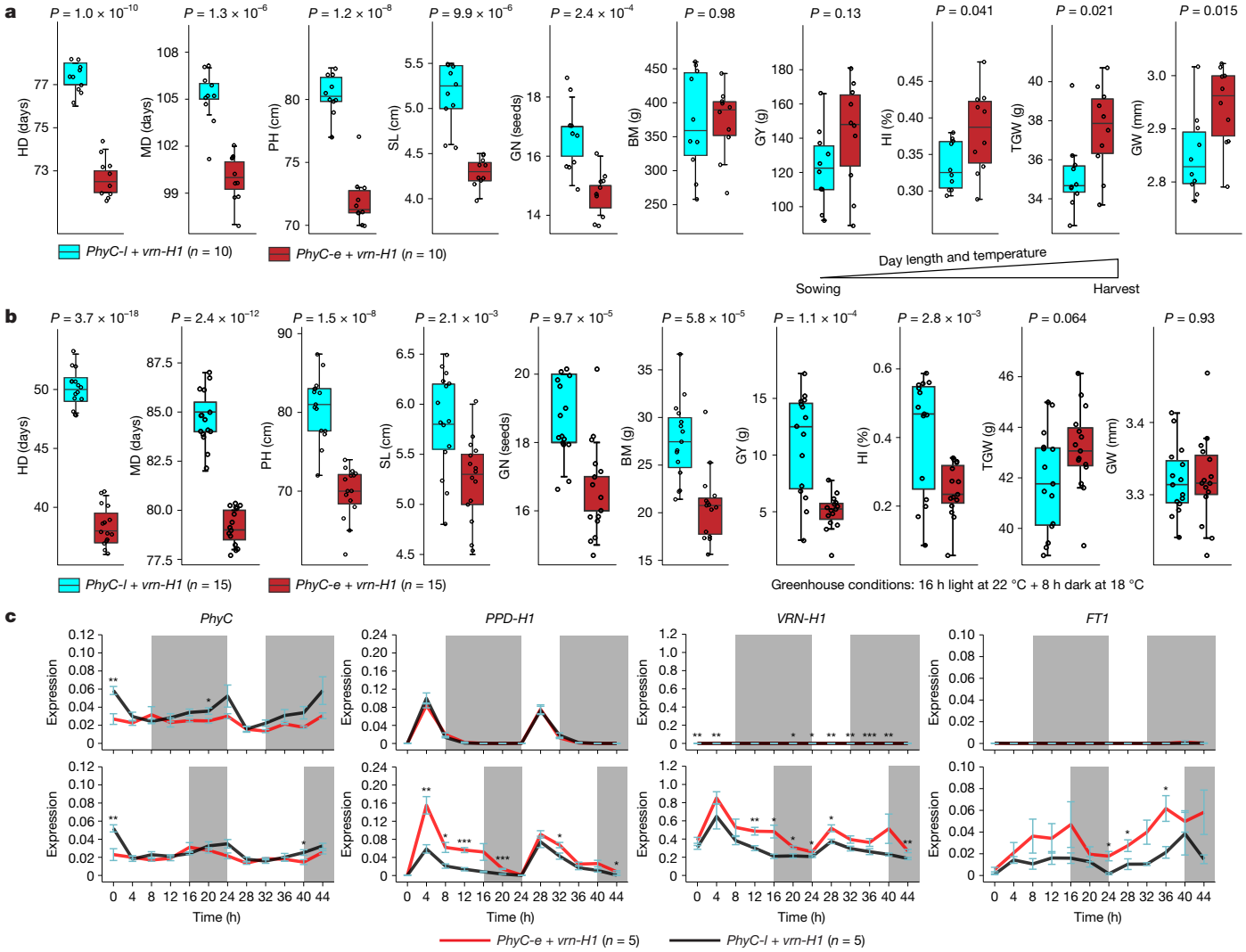


Fig. 4 | Haplotype combination *PhyC-e* + *vrn-H1* confers pleiotropic advantages under stressed conditions. a,**b**, Statistics of ten agronomic traits under field conditions (**a**) and greenhouse conditions (**b**). In the field trial, each genotype contained ten replicates in rows, and each row harvest served as a measurement. In the greenhouse experiment, 15 plants of each genotype were measured individually. Box plots show the 25–75% interval of raw value in the box, with central lines indicating the median and whiskers extending to the minimum and maximum values within 1.5× of the interquartile range. Each individual value (*n*) represents a biologically independent replicate. **c**, Transcriptional patterns of flowering regulation genes in *PhyC-e* + *vrn-H1* (red line) and *PhyC-l* + *vrn-H1* (black line) combinations under short-day and long-day conditions. Grey shading indicates the night-time duration. Data are presented as mean ± standard error (s.e.). Statistical significance was determined using a two-tailed *t*-test (*$P \leq 0.05$; **$P \leq 0.01$; ***$P \leq 0.001$; results that are not significant are not shown in the figures). BM, biomass; GY, grain yield; HI, harvest index.

Taken together, these findings explain why the *PhyC-e* haplotype rose to high frequency in Chinese modern varieties. In combination with the winter-type *vrn-H1*, it forms a preferred module that confers pleiotropic advantages without yield loss under double-season cropping system. Its enrichment in autumn-sown modern varieties reflects decades of unconscious selection for this haplotype module by breeders working to optimize the barley life cycle (Fig. 3c).

Base editing demonstrates causality

Sequence alignment of 2,058 PhyC homologues from more than 1,400 species across the plant kingdom revealed that the phenylalanine residue at the 380th amino acid is highly conserved (Fig. 5a and Supplementary Table 9). Sequence analysis of 1,051 wheat[35] and 2,231 barley[30] accessions revealed that the phenylalanine residue is universally conserved, with the sole exception being the derived serine substitution found in a subset of East Asian barley accessions. To further validate the effect of the T1139C substitution at *PhyC* on its function, we used adenine base editing to recreate the same substitution in modern varieties of barley and hexaploid wheat, which share a highly conserved regulatory framework governing photoperiod and vernalization responses during floral induction[9]. This approach precisely converted the codon 'TTC' (phenylalanine) to 'TCC' (serine) at the 380th amino acid of PhyC protein in its highly conserved GAF domain (Fig. 5b).

In barley, editing was performed in the spring-type Australian variety 'Vlamingh' (*PhyC-l* + *Vrn-H1*). Several independent T_0 plants carrying the targeted substitution were generated, and homozygous T_2 plants were advanced for phenotypic analysis (Supplementary Table 10). Under long-day greenhouse conditions, edited plants (*PhyC-e* + *Vrn-H1*) flowered and matured significantly earlier than wild-type controls, simultaneously with drawbacks in yield components (Fig. 5c,d), consistent with the performance of NILs carrying *PhyC-e* at the spring-type *Vrn-H1* background (Extended Data Fig. 7d,e). Heterozygous plants showed similar phenotypes to homozygotes, suggesting *PhyC-e* as a dominant flowering regulator (Extended Data Fig. 8a,b). In field trials, edited lines headed earlier and were shorter as well, confirming

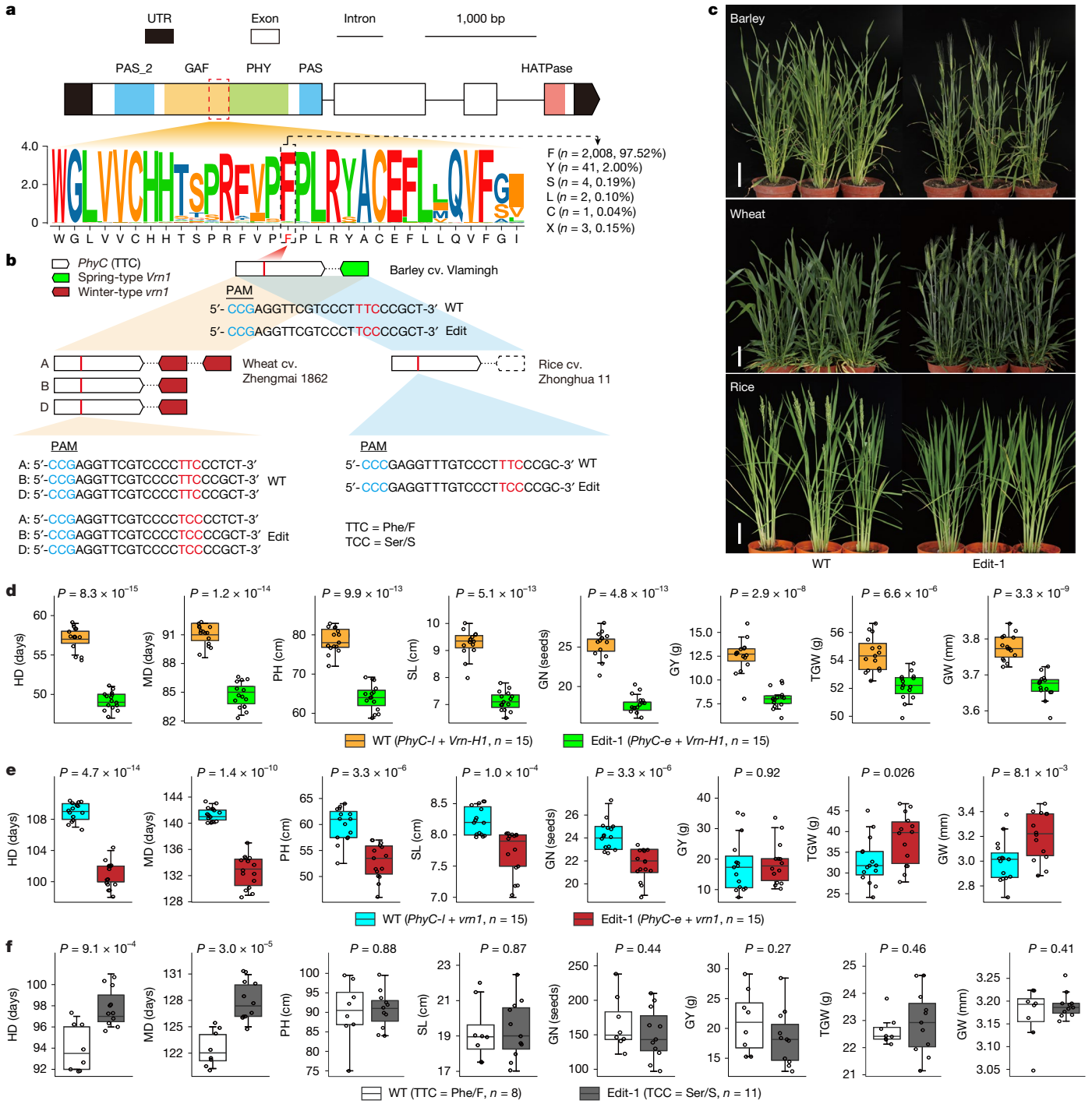


Fig. 5 | Base editing of *PhyC* in barley, wheat and rice. a, Gene structure of *PhyC* and conservation analysis at the target phenylalanine (F) site based on 2,059 PhyC homologous amino acid sequences from 1,499 species. Six variant residues (F, Y, S, L, C, X) were identified. **b**, The single-guide RNA and altered *PhyC* nucleotide sequences in barley, wheat and rice. Protospacer adjacent motif (PAM) sequences are highlighted in blue and target nucleotides are marked in red. **c**, Phenotype of base-edited homozygous mutant lines at the heading stage. **d**–**f**, Statistics of eight agronomic traits in barley (**d**), wheat (**e**) and rice (**f**). Box plots show the 25–75% interval of raw value in the box, with central lines indicating the median and whiskers extending to the minimum and maximum values within 1.5× of the interquartile range. Each individual value (*n*) represents a biologically independent replicate. Statistical significance was determined using a two-tailed *t*-test. HATPase, histidine kinase-like ATPase domain; GAF, cGMP-stimulated phosphodiesterase domain; PAS/PAS_2, Per-Arnt-Sim domain; PHY, phytochrome domain; UTR, untranslated region. Scale bar, 10 cm.

the consistency of the phenotype across environments (Extended Data Fig. 8c,d). Transcript profiling revealed elevated expression of *PPD-H1*, *FT1* and *VRN-H1* (Extended Data Fig. 8e), consistent with accelerated heading under long days. Notably, increases in the transcriptional abundance of *FT1* and *VRN-H1* were observed in *PhyC-e* compared with *PhyC-l* in a spring-type *Vrn-H1* background, whereas the increases in the winter-type *vrn-H1* background were not as large (Extended Data Fig. 8f).

In wheat, we generated the same substitution in the winter-type Chinese variety ‘Zhengmai 1862’ (*PhyC-l* + winter-type *vrn1* homologues). Because of its hexaploid genome, edits were desired at all three *PhyC* homologues (Supplementary Table 11). We obtained

homozygous triple-edited lines at the T_1 generation (Fig. 5b). When cultivated in pots under conditions mirroring the barley trial (Extended Data Fig. 7b), the edited wheat lines (*PhyC-e* + *vrn1*) headed and matured earlier than wild-type plants, with moderate reductions in spike length and grain number but no significant penalty to total grain yield (Fig. 5e). The yield compensation may arise from larger grain size, consistent with the performance of NILs carrying *PhyC-e* at the winter-type *vrn-H1* background (Fig. 4a). Under greenhouse conditions, the edited lines showed a similar performance (Extended Data Fig. 9a,b), as observed in barley NIL-set2 (Fig. 4b), accompanied by mild transcriptional induction of *FT1* gene (Extended Data Fig. 9c).

These results establish *PhyC-e* as a causal determinant of early flowering, with conserved function across Triticeae cereals. The consistent observations across NILs, natural cultivars and base-edited lines strengthen the conclusion that the F380S substitution accelerates flowering and maturity under long-day conditions, enabling crops to escape terminal heat stress. The *PhyC-e* + *vrn1* module achieved an optimal balance between maturity date and biomass accumulation by fine-tuning the transcriptional levels of key flowering-time regulators. Furthermore, these findings demonstrate how precision genome editing can resolve long-standing questions of causality in crop adaptation and opens avenues for targeted deployment of beneficial variants in Triticeae breeding.

Conservation across cereals

To further test the lineage specificity of the particular phenylalanine residue at the position 380 of PhyC, we extended editing experiments to the summer crop rice (*Oryza sativa*), in which the *VRN1* orthologue is absent (Fig. 5b). We introduced the F-to-S substitution on the *PhyC* orthologue in *Japonica* rice cultivar 'Zhonghua 11' (Supplementary Table 12). Edited plants showed delayed flowering in the summer trials (Fig. 5c,f), opposite to the effect observed in barley and wheat, and showed no effect on yield components (Fig. 5f). This divergence probably reflects differentiations in photoperiodic pathways between temperate and tropical or subtropical cereals, as rice is a short-day crop in which activated phytochrome suppresses flowering under long days, whereas Triticeae cereals are long-day species in which activated phytochrome promotes flowering. Thus, although the same substitution is functionally crucial across cereals, its phenotypic effect depends on species-specific photoperiodic response mechanisms.

Discussion

This study identifies and experimentally validates a conserved flowering-time module (Extended Data Fig. 10) that has been assembled and selected during modern breeding to enable adaptation to double-season cropping, and that can be reconstituted in other temperate cereals such as wheat. The evolutionary conservation of the affected residue, combined with the restricted geographic distribution of the derived haplotype, is consistent with the emergence and subsequent selection of a locally adaptive solution to intensive double-season cropping. A single amino acid change in *PhyC*, in combination with a winter-type *vrn-H1* haplotype, enables early flowering and maturation that align with the narrow autumn–spring cultivation window in central and eastern China. Crucially, we demonstrate causality through base editing in barley and wheat, establishing the functional conservation of this module across the Triticeae tribe. This moves beyond proof-of-concept to explain and recreate the adaptation module implemented in breeding. The contrasting effect in rice highlights the need to tailor flowering-time manipulations to the ecological and photoperiodic context of each crop.

Looking forward, our findings have implications extending beyond barley in China. As climate change accelerates[36], double-season cropping systems and other intensified rotations will become increasingly important for food security. Early flowering and heat escape, as mediated by the *PhyC-e* + *vrn-H1* module, illustrates how targeted manipulation of conserved pathways can provide robust adaptation strategies in cereals. Similar modules could be explored in other Triticeae cropping systems in which early flowering and stress escape are critical, such as barley grown in Mediterranean areas or wheat in high-latitude regions. More broadly, our study highlights the value of integrating historical genomics, field-based phenotyping and precision genome editing to resolve the genetic basis of crop adaptation. This integrative framework offers a model for designing climate-resilient Triticeae varieties tailored to the challenges of future agriculture.

Online content

Any methods, additional references, Nature Portfolio reporting summaries, source data, extended data, supplementary information, acknowledgements, peer review information; details of author contributions and competing interests; and statements of data and code availability are available at https://doi.org/10.1038/s41586-026-11187-y.

1. Dawson, I. K. et al. Barley: a translational model for adaptation to climate change. *New Phytol.* **206**, 913–931 https://doi.org/10.1111/nph.13266 (2015).
2. Gutaker, R. M. & Purugganan, M. D. Adaptation and the geographic spread of crop species. *Annu. Rev. Plant Biol.* **75**, 679–706 https://doi.org/10.1146/annurev-arplant-060223-030954 (2024).
3. Smith, M. E. et al. Increasing crop rotational diversity can enhance cereal yields. *Commun. Earth Environ.* **4**, 89 https://doi.org/10.1038/s43247-023-00746-0 (2023).
4. Yang, X. et al. Diversifying crop rotation increases food production, reduces net greenhouse gas emissions and improves soil health. *Nat. Commun.* **15**, 198 https://doi.org/10.1038/s41467-023-44464-9 (2024).
5. Harlan, J. R. & Zohary, D. Distribution of wild wheats and barley. *Science* **153**, 1074–1080 https://doi.org/10.1126/science.153.3740.1074 (1966).
6. Zohary, D., Hopf, M. & Weiss, E. *Domestication of Plants in the Old World: The Origin and Spread of Domesticated Plants in Southwest Asia, Europe, and the Mediterranean Basin* (Oxford Univ. Press, 2012).
7. Liu, X. et al. Journey to the east: diverse routes and variable flowering times for wheat and barley en route to prehistoric China. *PLoS ONE* **12**, e0187405 https://doi.org/10.1371/journal.pone.0187405 (2017).
8. Jones, H. et al. Population-based resequencing reveals that the flowering time adaptation of cultivated barley originated east of the Fertile Crescent. *Mol. Biol. Evol.* **25**, 2211–2219 https://doi.org/10.1093/molbev/msn167 (2008).
9. Campoli, C. & von Korff, M. Genetic control of reproductive development in temperate cereals. *Adv. Bot. Res.* **72**, 131–158 https://doi.org/10.1016/B978-0-12-417162-6.00005-5 (2014).
10. Trevaskis, B., Bagnall, D. J., Ellis, M. H., Peacock, W. J. & Dennis, E. S. MADS box genes control vernalization-induced flowering in cereals. *Proc. Natl Acad. Sci. USA* **100**, 13099–13104 https://doi.org/10.1073/pnas.1635053100 (2003).
11. Yan, L. et al. Positional cloning of the wheat vernalization gene *VRN1*. *Proc. Natl Acad. Sci. USA* **100**, 6263–6268 https://doi.org/10.1073/pnas.0937399100 (2003).
12. Yan, L. et al. The wheat *VRN2* gene is a flowering repressor down-regulated by vernalization. *Science* **303**, 1640–1644 https://doi.org/10.1126/science.1094305 (2004).
13. Yan, L. et al. The wheat and barley vernalization gene *VRN3* is an orthologue of *FT*. *Proc. Natl Acad. Sci. USA* **103**, 19581–19586 https://doi.org/10.1073/pnas.0607142103 (2006).
14. Turner, A., Beales, J., Faure, S., Dunford, R. P. & Laurie, D. A. The pseudo-response regulator *Ppd-H1* provides adaptation to photoperiod in barley. *Science* **310**, 1031–1034 https://doi.org/10.1126/science.1117619 (2005).
15. Kikuchi, R., Kawahigashi, H., Ando, T., Tonooka, T. & Handa, H. Molecular and functional characterization of *PEBP* genes in barley reveal the diversification of their roles in flowering. *Plant Physiol.* **149**, 1341–1353 https://doi.org/10.1104/pp.108.132134 (2009).
16. Russell, J. et al. Exome sequencing of geographically diverse barley landraces and wild relatives gives insights into environmental adaptation. *Nat. Genet.* **48**, 1024–1030 https://doi.org/10.1038/ng.3612 (2016).
17. Marden, E., Sackville Hamilton, R., Halewood, M. & McCouch, S. International agreements and the plant genetics research community: a guide to practice. *Proc. Natl Acad. Sci. USA* **120**, e2205773119 https://doi.org/10.1073/pnas.2205773119 (2023).
18. Zhang, J. & Zhang, W. Tracing sources of dwarfing genes in barley breeding in China. *Euphytica* **131**, 285–293 https://doi.org/10.1023/A:1024032732443 (2003).
19. Nishida, H. et al. *Phytochrome C* is a key factor controlling long-day flowering in barley. *Plant Physiol.* **163**, 804–814 https://doi.org/10.1104/pp.113.222570 (2013).
20. Pankin, A. et al. Mapping-by-sequencing identifies *HvPHYTOCHROME C* as a candidate gene for the *early maturity 5* locus modulating the circadian clock and photoperiodic flowering in barley. *Genetics* **198**, 383–396 https://doi.org/10.1534/genetics.114.165613 (2014).
21. Alvarez, M. A. et al. *EARLY FLOWERING 3* interactions with *PHYTOCHROME B* and *PHOTOPERIOD1* are critical for the photoperiodic regulation of wheat heading time. *PLoS Genet.* **19**, e1010655 https://doi.org/10.1371/journal.pgen.1010655 (2023).
22. Gao, M. et al. Phytochromes transmit photoperiod information via the evening complex in *Brachypodium*. *Genome Biol.* **24**, 256 https://doi.org/10.1186/s13059-023-03082-w (2023).

23. Woods, D. P. et al. *PHYTOCHROME C* regulation of photoperiodic flowering via *PHOTOPERIOD1* is mediated by *EARLY FLOWERING 3* in *Brachypodium distachyon*. *PLoS Genet.* **19**, e1010706 https://doi.org/10.1371/journal.pgen.1010706 (2023).
24. Xue, C. et al. Tuning plant phenotypes by precise, graded downregulation of gene expression. *Nat. Biotechnol.* **41**, 1758–1764 https://doi.org/10.1038/s41587-023-01707-w (2023).
25. Li, B., Sun, C., Li, J. & Gao, C. Targeted genome-modification tools and their advanced applications in crop breeding. *Nat. Rev. Genet.* **25**, 603–622 https://doi.org/10.1038/s41576-024-00720-2 (2024).
26. Luo, S. et al. *China Barley Variety Directory (1950–1985)* (Agriculture Press, 1989).
27. Zhang, J. et al. *China Barley Variety Directory (1986–2015)* (China Agricultural Science and Technology Press, 2018).
28. Zeng, X. et al. Origin and evolution of qingke barley in Tibet. *Nat. Commun.* **9**, 5433 https://doi.org/10.1038/s41467-018-07920-5 (2018).
29. Milner, S. G. et al. Genebank genomics highlights the diversity of a global barley collection. *Nat. Genet.* **51**, 319–326 https://doi.org/10.1038/s41588-018-0266-x (2019).
30. Jayakodi, M. et al. Structural variation in the pangenome of wild and domesticated barley. *Nature* **636**, 654–662 https://doi.org/10.1038/s41586-024-08187-1 (2024).
31. Taketa, S. et al. Barley grain with adhering hulls is controlled by an ERF family transcription factor gene regulating a lipid biosynthesis pathway. *Proc. Natl Acad. Sci. USA* **105**, 4062–4067 https://doi.org/10.1073/pnas.0711034105 (2008).
32. Komatsuda, T. et al. Six-rowed barley originated from a mutation in a homeodomain-leucine zipper I-class homeobox gene. *Proc. Natl Acad. Sci. USA* **104**, 1424–1429 https://doi.org/10.1073/pnas.0608580104 (2007).
33. Chono, M. et al. A semidwarf phenotype of barley *uzu* results from a nucleotide substitution in the gene encoding a putative brassinosteroid receptor. *Plant Physiol.* **133**, 1209–1219 https://doi.org/10.1104/pp.103.026195 (2003).
34. Hemming, M. N., Fieg, S., Peacock, W. J., Dennis, E. S. & Trevaskis, B. Regions associated with repression of the barley (*Hordeum vulgare*) *VERNALIZATION1* gene are not required for cold induction. *Mol. Genet. Genomics* **282**, 107–117 https://doi.org/10.1007/s00438-009-0449-3 (2009).
35. Cheng, S. et al. Harnessing landrace diversity empowers wheat breeding. *Nature* **632**, 823–831 https://doi.org/10.1038/s41586-024-07682-9 (2024).
36. Hermanson, L. et al. WMO global annual to decadal climate update: a prediction for 2021–25. *Bull. Am. Meteorol. Soc.* **103**, E1117–E1129 https://doi.org/10.1175/BAMS-D-20-0311.1 (2022).
37. Guo, Y. et al. A haplotype-based evolutionary history of barley domestication. *Nature* **647**, 680–688 https://doi.org/10.1038/s41586-025-09533-7 (2025).

Publisher's note Springer Nature remains neutral with regard to jurisdictional claims in published maps and institutional affiliations.

Springer Nature or its licensor (e.g. a society or other partner) holds exclusive rights to this article under a publishing agreement with the author(s) or other rightsholder(s); author self-archiving of the accepted manuscript version of this article is solely governed by the terms of such publishing agreement and applicable law.

© The Author(s), under exclusive licence to Springer Nature Limited 2026

Methods

Barley landraces and cultivars

Chinese barley researchers have compiled two volumes of the 'China Barley Variety Directory'[26,27], documenting 511 barley landraces and cultivars that served as main production varieties in China from 1940s to 2015. For this study, we obtained 421 accessions (82.39% of the documented varieties) from the National Crop Genebank of China and collaborating breeders, representing an 80-year temporal range and nationwide geographic distribution. In addition, we included 38 cultivars released before 2015 but not included in the two directories, 46 modern cultivars registered after 2015, along with 27 introduced varieties (exotic lines). These exotic lines originated primarily from Europe, North America and Australia, with a few from Asia and Africa, and represented both historical and modern cultivars with diverse genetic backgrounds (Supplementary Table 1). This includes 186, 155 and 164 representative varieties that were popularly planted in China during the 1940s–1950s (designated 'CN1940&50'), 1960s–1980s ('CN60&70&80') and 1990s–2010s ('CN90&00&10'), respectively. This diverse panel encompassed the full spectrum of barley variations in growth habit, spike row type pattern, hull adherence and end-use (malting, feed or food). These accessions underwent two cycles of seed multiplication using the single-seed descent method before conducting subsequent field trials.

Field trials and statistical analysis

Six independent trials were carried out across two growing seasons (2020–2021 and 2021–2022) at three geographically distinct locations, namely Xinxiang (113° 92′ E, 35° 30′ N, 79 m elevation) in Henan Province, Yancheng (120° 16′ E, 33° 35′ N, 5 m elevation) in Jiangsu Province and Kunming (102° 72′ E, 25° 04′ N, 2,136 m elevation) in Yunnan Province, China. All trials followed an autumn-sown schedule, with sowing dates in mid-October for Xinxiang, late-October for Yancheng and early-November for Kunming. We used a randomized complete block design with two to three replicates per genotype at each location. Each replicate consisted of 2 rows of 1.5 m in length and spaced 25 cm apart, with 65 seeds sown per row.

We evaluated ten key agronomic traits: the heading date (recorded when 50% of tillers in a plot had fully emerged spikes), maturity date (recorded when 80% of tillers showed natural senescence and grains reaching the late dough stage), plant height, spike length, spike density, grain number per spike, grain length, grain width, grain length-to-width ratio and thousand-grain weight. For four traits including plant height, spike length, spike density and grain number, the main tiller and corresponding spike from ten randomly selected plants per replicate were measured. At harvest, roughly 300 grains per replicate were subjected to measurement of the grain characteristics using the SC-G automatic grain analyser (Wanshen Testing Technology Co.). Statistical analyses were conducted in R software suite (v.4.2.3; https://www.r-project.org/). For each trait in individual trials, we used the adjusted mean values from replicates for subsequent analysis. The best linear unbiased estimators for traits of each genotype across several trials was calculated using the lme4 v.1.1.37 (ref. 38). Statistical differences among genotypic groups were examined using one-way analysis of variance (ANOVA), with Fisher's least significant difference tests for post hoc pairwise comparisons ($P = 0.05$).

WGS, reads mapping and variant calling

Young leaves from individual seedlings of each genotype were harvested for genomic DNA extraction using the cetyltrimethylammonium bromide method. DNA quality was assessed by agarose gel electrophoresis, Nanodrop spectrophotometer (ThermoFisher) and Qubit DNA Assay Kit in Qubit v.3.0 Flurometer (Invitrogen). The sequencing library was prepared using the VAHTS Universal Plus DNA Library Prep Kit (Vazyme) according to the manufacturer's protocol. After quality assessment, qualified libraries were pooled, circularized and processed into DNA nanoballs. The DNA nanoballs were then loaded onto sequencing chips and processed on the DNBSEQ-T7 platform (MGI) to generate 150-base-pair (bp) paired-end (PE150) reads. Adapters and low-quality bases in raw reads were trimmed using cutadapt v.3.3 (ref. 39) with a minimum read length of 30 bp. Clean reads were aligned to the barley reference genome 'MorexV3' (ref. 40) using Minimap2 v.2.20 (ref. 41) with default parameters. The output was converted to binary alignment map (BAM) format and sorted using SAMtools (v.1.9)[42], and duplicates were marked with NovoSort (v.3.06.05) (http://www.novocraft.com). BCFtools v.1.9 (ref. 42) using mpileup and call functions were deployed for variant calling with the parameters (-q 20 -Q 20 --excl-flags 3332). Bi-allelic variants were recalled based on read depth using a custom awk script that was adopted from an online source (https://github.com/whyeonc/vcf_filtering/tree/main), with the following criteria: (1) homozygous and heterozygous calls were supported with a minimum of two and four reads, respectively; (2) SNPs were accepted only if they had less than 10% missing data and less than 10% heterozygous genotype calls; and (3) the minor allele frequency (MAF) was at least 0.01.

Population diversity analysis

Principal component analysis of the 532 cultivars was conducted by merging their variant call format (vcf) data with the published variant matrix of 19,778 domesticated barley accessions derived from genotyping-by-sequencing[29], followed by combined analysis using PLINK v.1.9 (ref. 43). For population structure analysis, the vcf of the 532 cultivars was integrated with the variant matrix of the global core germplasm CORE1000 dataset[30]. The merged variants were filtered using the same custom awk script as mentioned. Genome-wide effective variants were estimated by pruning variants with $r^2 \geq 0.1$, setting with 1-kb sliding window and 100-bp step size in PLINK v.1.9 (ref. 43). Qualified variants were subjected to population structure analysis using ADMIXTURE v.1.3.0 (ref. 44), with ten different random seeds at each K estimate, and the ancestry proportions (Q) generated from ten replications were integrated by CLUMPP v.1.1.2 (ref. 45). A neighbour-joining tree was constructed on the basis of pairwise genetic distances using TreeBeST v.1.9.2 (ref. 46) with 1,000 bootstrap replicates. F_{st} values between diversity groups were calculated using VCFtools v.0.1.16 (ref. 47) with a window size of 20 kb and a step window of 10 kb. The nucleotide diversity (π) within each group was estimated using custom Perl scripts (available at https://sourceforge.net/projects/origin-of-qingke-barley/files/) as described in ref. 28.

Foundation lines identification

The genomic-based germplasm network (GGNet) was constructed by analysing the gIBD segments among all pairwise combinations of the 532 varieties using the ggComp pipeline with 1 Mb windows[48]. The resulting bam and vcf files from reads mapping and variant calling were processed to calculate gIBD for each pair of accessions. These gIBD values were transformed into a distance matrix and visualized as a clustered network to Cytoscape v.3.10.1 (ref. 49). The nodes represent particular accessions that were sized according to their network degree and edges indicating relationships with 50% or more gIBD. Ancestral haplotype groups were delineated through the IntroBlocker pipeline with 1 Mb windows[50], to characterize historical recombination patterns. Watterson's theta (θw)[51] and the Shannon diversity index[52] were calculated with a custom Perl script[37] based on IntroBlocker haplotype matrices.

GWAS

We conducted genome-wide association studies (GWAS) for each of the 10 agronomic traits among 532 cultivars using rigorously filtered SNPs (MAF ≥ 0.05 and missing data ≤0.1), with genotype imputation performed using Beagle v.5.4 with default parameters[53]. The analysis incorporated both trial-specific adjusted means and best linear

unbiased estimation (BLUE) values for each trial. GWAS was conducted with a mixed linear model in gemma v.0.98.5 (ref. 54) that accounted for population structure by including the top three principal components as covariates. We maintained analytical consistency by using the same linkage disequilibrium-pruned SNPs ($r^2 < 0.1$) from population structure analysis, establishing a stringent significance threshold ($P < 1 \times 10^{-6}$; Benjamini–Hochberg false discovery rate 0.05) for identifying robust marker–trait associations.

Haplotype analysis

For the *PhyC* gene, sequence polymorphisms across the 532 cultivars, CORE1000, SHAPE_cv, WBDC and WILD100 panels[30,37] were extracted from the emerged variant metrics using a custom Perl script. Imputed sequences were aligned using Sequencher v.4.8 (Gene Codes Corporation), and exported files were used for defining haplotypes by DNASP v.6.12.03 (ref. 55). Median-joining networks of haplotypes were constructed and visualized by PopART v.1.7 (ref. 56). For the *VRN-H1* gene, the sequence length polymorphic markers reported in ref. 57 were deployed for genotyping and identifying haplotypes of *VRN-H1* among the 532 varieties. Meanwhile, 2,231 whole-genome sequencing (WGS) data including the 532 cultivars was mapping to the wild barley reference genome of FT333 (ref. 30), which carries the winter-type *vrn-H1* (full-length intron 1) fragment. The read depth in intron 1 of *VRN-H1* was calculated using SAMtools v.1.9 (ref. 42).

Haplotype age was estimated using GEVA v.1 (ref. 58) based on 1,017 barley accessions, comprising WBDC[37], CORE200 (ref. 30) and 532 cultivars from this study. The filtered SNP dataset generated from the FT333-based mapping and variant-calling pipeline described above, was phased using Beagle v.5.4 (ref. 53). GEVA was run using the joint mutation-recombination clock model, and allele ages were estimated using the 'estimate.R' script provided with the GEVA package. Allele ages were estimated across combinations of three mutation rates and two recombination rates. Three mutation rates reported in cereals were used: 6.50×10^{-9} substitutions per site per generation for rice[59], 1.60×10^{-8} for wheat[60], 3.02×10^{-8} for maize calculated as the mean of the minimum (2.17×10^{-8}) and maximum (3.87×10^{-8}) estimates reported in ref. 61. Two recombination rates reported for barley[62] were used: 4.50×10^{-9} per site per generation, corresponding to the genome-wide median, and 3.83×10^{-8} per site per generation, calculated as the mean of the minimum (1.21×10^{-8}) and maximum (6.45×10^{-8}) rates reported for distal chromosomal regions. Ten replicate analyses were performed for each parameter combination using different random seeds. As controls, the 50 nearest SNPs on either side of the causal *PhyC-e* (T1139C) were selected if they were present in *PhyC-e* accessions and had a 0 < alternative allele frequency ≤ 50% in whole panel.

Haplotype block analysis was conducted with custom Perl scripts as described in ref. 37 (available at https://github.com/guoyu-meng/barley-haplotype-script). SNP genotypes were imputated and phased with Beagle v.5.4 (ref. 53), and XP-CLR scores were calculated using a Python implementation of XP-CLR v.1.1.2 (ref. 63) (https://github.com/hardingnj/xpclr) using a sliding window and step size of 20 kb each.

Conserved motif analysis

A total of 2,059 protein sequences of PhyC homologues from 1,499 species were extracted from the non-redundant protein sequence database (nr database), using PROVEAN v.1.1.5 software[64] with the full-length PhyC protein as the query. The conserved motif was visualized using WebLogo (https://weblogo.threeplusone.com).

Development of NILs and phenotyping

A cross-pollination between the germplasm PY01574 (*PhyC-l*/late flowering + *Vrn-H1* haplotype V1-4/spring-type) and the variety 'Hua30' (NDT-258; *PhyC-e*/early flowering + *vrn-H1*/winter-type) was carried out to generate NILs of various haplotypes combinations. We developed the codominant polymorphic markers for *PhyC* and *VRN-H1* (Supplementary Table 13), respectively, and screened 1,000 F_2 individuals to identify recombinants between the 2 genes. We used the *VRN-H1* marker together with newly developed two KASP markers (5H525919559 and 5H526488386) to narrow down the target interval in F_3 population. From the F_4 to F_7 generations, two flanking markers *VRN-H1* and 5H526488386 as well as a cosegregating marker *PhyC*, were used to select the target genomic region. Advanced F_8 homozygous segregants, both '*PhyC-l* + *Vrn-H1*' and '*PhyC-e* + *Vrn-H1*' (NIL-set1), were obtained by means of self-pollination and marker-assisted selection.

Furthermore, a crossing between the germplasm 'PY00891' (*PhyC-l* + *Vrn-H1* haplotype V1-6/spring-type) and the variety 'Dan2' (NDT-242; *PhyC-e* + *vrn-H1*) was carried out. A total of 192 F_3 individuals were genotyped using the *PhyC* and *VRN-H1* codominant markers. From the F_4 to F_6 generations, two flanking markers *VRN-H1* and 5H525230748, as well as a cosegregating marker *PhyC* were used for tracking the target region. F_7 homozygous recombinants of both '*PhyC-l* + *vrn-H1*' and '*PhyC-e* + *vrn-H1*' (NIL-Set2) were obtained.

These two pairs of NILs were further genotyped using WGS to finely characterize the recombination breakpoints and genomic heterozygosity, followed by seed multiplication through self-pollination in greenhouse. Phenotypic evaluations were carried out under controlled greenhouse conditions and many field environments including autumn sown (Xinxiang, 2024–2025; Extended Data Fig. 7a) or early-spring sown (Beijing, 2025; Extended Data Fig. 7b).

Adenine base editing in barley, wheat and rice

Sequences of the *PhyC* orthologues in wheat and rice were retrieved from the Ensembl Plants database (https://plants.ensembl.org/index.html). For targeted base substitution, we used an adenine base editing system with species-specific target sequences in barley, wheat and rice, respectively. The *Agrobacterium tumefaciens*-mediated transformation was conducted in the barley cultivar 'Vlamingh' and wheat cultivar 'Zhengmai 1862' at the National Research Center of Plant Transgenic Technology (Institute of Crop Sciences, Chinese Academy of Agricultural Sciences), and rice cultivar 'Zhonghua 11' at the Edgene Biotech. Co. (Wuhan). The regenerated plants and homozygous offspring lines were genotyped through Sanger sequencing with gene-specific primers (Supplementary Table 13). Phenotypic characterization of edited lines was performed under greenhouse conditions and controlled spring-sown field conditions (Beijing, 2025).

Transcriptional quantification of flowering-time regulatory genes

For barley, gene expression analysis was performed through controlled experiments using NIL-set2, and the barley edited line NJ292-*PhyC-e* and its sibling line NJ292-*PhyC-l*. Germinated seeds were individually sown in culture pots and treated for 4 days at 4 °C for breaking dormancy, followed by culturing under either long-day (16 h light, 20 °C; 8 h dark, 16 °C) or short-day (8 h light, 20 °C; 16 h dark, 16 °C) conditions for 28 days in growth chambers. For temporal expression profiling, leaves were harvested from each plant at 4-h intervals over 48 h beginning at the light period (time point T_0).

For wheat, the wild-type cultivar 'Zhengmai 1862' (*PhyC-l* + *vrn1*) and edited line (*PhyC-e* + *vrn1*) were used. Following seed dormancy release, plants were vernalizated at 4 °C for 6 weeks and then grown under long-day conditions (16 h light at 22 °C and 8 h dark at 18 °C) for 28 days in growth chambers. For temporal expression profiling, leaf samples were collected at 4-h intervals over a 24 h period starting at T_0.

Total RNA was extracted using the Trizol reagent (Genebetter Co.), and complementary DNA (cDNA) synthesis was performed using the HiScript III 1st Strand cDNA Synthesis Kit (Vazyme). Quantitative real-time PCR with reverse transcription was performed using gene-specific primers (Supplementary Table 13) with SYBR Green reagent (Vazyme) on the QuantStudio 6 Flex Real-Time system (ThermoFisher Scientific).

Reporting summary

Further information on research design is available in the Nature Portfolio Reporting Summary linked to this article.

Data availability

Sequence data for 510 accessions generated in this study have been deposited at the China National Center for Bioinformation under BioProject ID PRJCA049684. Sequence data for an extra 22 accessions were obtained from the National Center for Biotechnology Information (NCBI) under BioProject ID PRJNA417220. Accession codes for all individual accessions are listed in Supplementary Table 2. The NCBI non-redundant protein database (nr) version 4 was used for protein sequence annotation (https://ftp.ncbi.nih.gov/blast/db/v4/). Source data are provided with this paper.

Code availability

The shell and Perl scripts used in this study are available at GitHub (https://github.com/guoyu-meng/barley-haplotype-script). Further in-house Perl and shell scripts for read mapping, variant calling, filtering and annotation, and population genetic analyses are available at SourceForge (https://sourceforge.net/projects/origin-of-qingke-barley/files/).

38. Bates, D., Mächler, M., Bolker, B. & Walker, S. Fitting linear mixed-effects models using lme4. *J. Stat. Softw.* **67**, 1–48 https://doi.org/10.18637/jss.v067.i01 (2015).
39. Martin, M. Cutadapt removes adapter sequences from high-throughput sequencing reads. *EMBnet J.* **17**, 3 https://doi.org/10.14806/ej.17.1.200 (2011).
40. Mascher, M. et al. Long-read sequence assembly: a technical evaluation in barley. *Plant Cell* **33**, 1888–1906 https://doi.org/10.1093/plcell/koab077 (2021).
41. Li, H. Minimap2: pairwise alignment for nucleotide sequences. *Bioinformatics* **34**, 3094–3100 https://doi.org/10.1093/bioinformatics/bty191 (2018).
42. Danecek, P. et al. Twelve years of SAMtools and BCFtools. *Gigascience* **10**, giab008 https://doi.org/10.1093/gigascience/giab008 (2021).
43. Purcell, S. et al. PLINK: a tool set for whole-genome association and population-based linkage analyses. *Am. J. Hum. Genet.* **81**, 559–575 https://doi.org/10.1086/519795 (2007).
44. Alexander, D., Novembre, J. & Lange, K. Fast model-based estimation of ancestry in unrelated individuals. *Genome Res.* **19**, 1655–1664 https://doi.org/10.1101/gr.094052.109 (2009).
45. Jakobsson, M. & Rosenberg, N. A. CLUMPP: a cluster matching and permutation program for dealing with label switching and multimodality in analysis of population structure. *Bioinformatics* **23**, 1801–1806 https://doi.org/10.1093/bioinformatics/btm233 (2007).
46. Vilella, A. J. et al. EnsemblCompara GeneTrees: complete, duplication-aware phylogenetic trees in vertebrates. *Genome Res.* **19**, 327–335 https://doi.org/10.1101/gr.073585.107 (2009).
47. Danecek, P. et al. The variant call format and VCFtools. *Bioinformatics* **27**, 2156–2158 https://doi.org/10.1093/bioinformatics/btr330 (2011).
48. Yang, Z. et al. ggComp enables dissection of germplasm resources and construction of a multiscale germplasm network in wheat. *Plant Physiol.* **188**, 1950–1965 https://doi.org/10.1093/plphys/kiac029 (2022).
49. Shannon, P. et al. Cytoscape: a software environment for integrated models of biomolecular interaction networks. *Genome Res.* **13**, 2498–2504 https://doi.org/10.1101/gr.1239303 (2003).
50. Wang, Z. et al. Dispersed emergence and protracted domestication of polyploid wheat uncovered by mosaic ancestral haploblock inference. *Nat. Commun.* **13**, 3891 https://doi.org/10.1038/s41467-022-31581-0 (2022).
51. Watterson, G. On the number of segregating sites in genetical models without recombination. *Theor. Popul. Biol.* **7**, 256–276 https://doi.org/10.1016/0040-5809(75)90020-9 (1975).
52. Spellerberg, I. F. & Fedor, P. J. A tribute to Claude Shannon (1916-2001) and a plea for more rigorous use of species richness, species diversity and the 'Shannon–Wiener' index. *Global Ecol. Biogeogr.* **12**, 177–179 https://doi.org/10.1046/j.1466-822X.2003.00015.x (2003).
53. Browning, S. R. & Browning, B. L. Rapid and accurate haplotype phasing and missing-data inference for whole-genome association studies by use of localized haplotype clustering. *Am. J. Hum. Genet.* **81**, 1084–1097 https://doi.org/10.1086/521987 (2007).
54. Zhou, X. & Stephens, M. Genome-wide efficient mixed-model analysis for association studies. *Nat. Genet.* **44**, 821–824 https://doi.org/10.1038/ng.2310 (2012).
55. Rozas, J. et al. DnaSP 6: DNA sequence polymorphism analysis of large data sets. *Mol. Biol. Evol.* **34**, 3299–3302 https://doi.org/10.1093/molbev/msx248 (2017).
56. Leigh, J. W. & Bryant, D. PopART: full-feature software for haplotype network construction. *Methods Ecol. Evol.* **6**, 1110–1116 https://doi.org/10.1111/2041-210X.12410 (2015).
57. Dondup, D. et al. Allelic variation and geographic distribution of vernalization genes *HvVRN1* and *HvVRN2* in Chinese barley germplasm. *Mol. Breed.* **36**, 11 https://doi.org/10.1007/s11032-016-0434-6 (2016).
58. Albers, P. K. & McVean, G. Dating genomic variants and shared ancestry in population-scale sequencing data. *PLoS Biol.* **18**, e3000586 https://doi.org/10.1371/journal.pbio.3000586 (2020).
59. Meyer, R. S. et al. Domestication history and geographical adaptation inferred from a SNP map of African rice. *Nat. Genet.* **48**, 1083–1088 https://doi.org/10.1038/ng.3633 (2016).
60. Dvorak, J. et al. Molecular characterization of a diagnostic DNA marker for domesticated tetraploid wheat provides evidence for gene flow from wild tetraploid wheat to hexaploid wheat. *Mol. Biol. Evol.* **23**, 1386–1396 https://doi.org/10.1093/molbev/msl004 (2006).
61. Yang, N. et al. Contributions of *Zea mays* subspecies *mexicana* haplotypes to modern maize. *Nat. Commun.* **8**, 1874 https://doi.org/10.1038/s41467-017-02063-5 (2017).
62. Casale, F. et al. Genomic prediction of the recombination rate variation in barley—a route to highly recombinogenic genotypes. *Plant Biotechnol. J.* **20**, 676–690 https://doi.org/10.1111/pbi.13746 (2022).
63. Chen, H., Patterson, N. & Reich, D. Population differentiation as a test for selective sweeps. *Genome Res.* **20**, 393–402 https://doi.org/10.1101/gr.100545.109 (2010).
64. Choi, Y. & Chan, A. P. PROVEAN web server: a tool to predict the functional effect of amino acid substitutions and indels. *Bioinformatics* **31**, 2745–2747 https://doi.org/10.1093/bioinformatics/btv195 (2015).

Acknowledgements We acknowledge the National Crop Genebank of China for providing seeds of barley accessions and the Core Facility Platform at the Institute of Crop Sciences, Chinese Academy of Agricultural Sciences (ICS-CAAS) for assistance with Sanger sequencing; C. Wang, S. Zhou, Q. He and Z. Wang from ICS-CAAS for advice on bioinformatics analysis; X. Ye and K. Wang from ICS-CAAS for transformation service; H. Guan and L. Yan from ICS-CAAS for technical support and B. Keller from the University of Zurich and S. Krattinger from King Abdullah University of Science and Technology for critical reading.

Author contributions Conception development: P.Y. Collection of germplasm resources: P.Y., J.Z. and N.S. Selection of barley accessions for sequencing: P.Y., C.J. and G.G. Sequence data analysis: G.G., Y.G., M.J. and J.-W.F. Field trials and phenotyping: G.G., C.J., W.W., C.A., M.S., C.C., X.X., H.Y., Y.Z. and H.S. Sequence data management and submission: G.G. Analysis of diversity in *PhyC* and *VRN-H1* genes: G.G. and Y.G. NIL development and phenotyping: G.G., C.J., W.W., J.W. and J.L. Adenine base editing and phenotyping: J.K., G.G., W.W., X.L. and W.Z. Protein structure modelling: A.S.C. and G.G. Article preparation: P.Y., G.G., C.J. and M.M. All authors read and approved the final paper.

Funding This work was supported by the State Key Laboratory of Crop Gene Resources and Breeding (grant no. S2026QZ05), Fundamental Research Funds for Central Non-Profit of CAAS (grant no. Y2025YC01) and Agricultural Science and Technology Innovation Program of CAAS (grant no. 01-ICS-03) to P.Y., the Mobility Program of the Sino-German Center for Research Promotion (grant no. M-0440) to P.Y. and M.M., and the National Natural Science Foundation of China (grant no. 32472148 to C.J. and 32241041 to J.K.).

Competing interests A patent application (Chinese patent application no. 202610703476.4) covering early-heading wheat and barley materials and their generation methods and applications has been filed by the Institute of Crop Sciences, Chinese Academy of Agricultural Sciences. P.Y., G.G., C.J., W.W. and J.K. are inventors on this patent application.

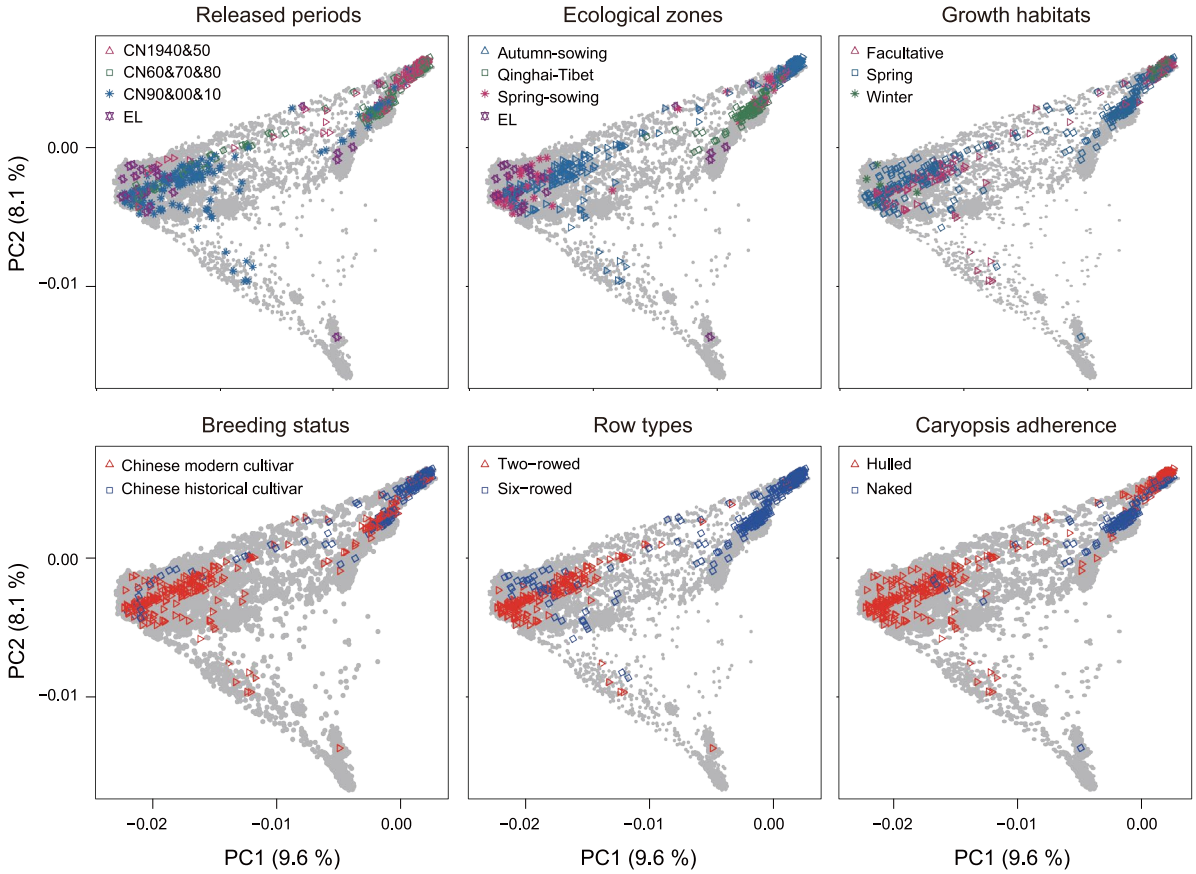
Additional information

Supplementary information The online version contains supplementary material available at https://doi.org/10.1038/s41586-026-11187-y.

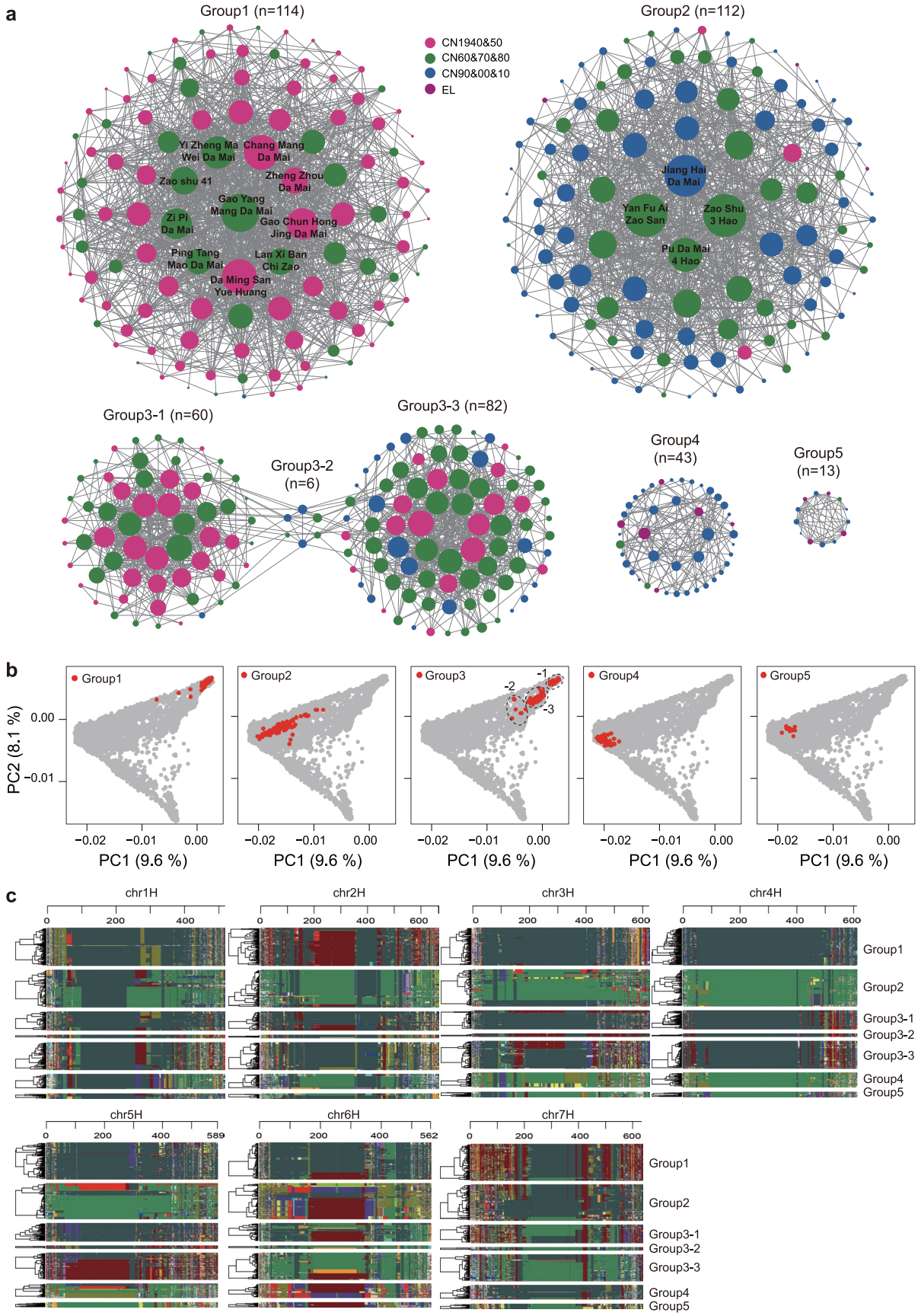
Correspondence and requests for materials should be addressed to Ping Yang.

Peer review information *Nature* thanks the anonymous reviewers for their contribution to the peer review of this work. Peer reviewer reports are available.

Reprints and permissions information is available at http://www.nature.com/reprints.

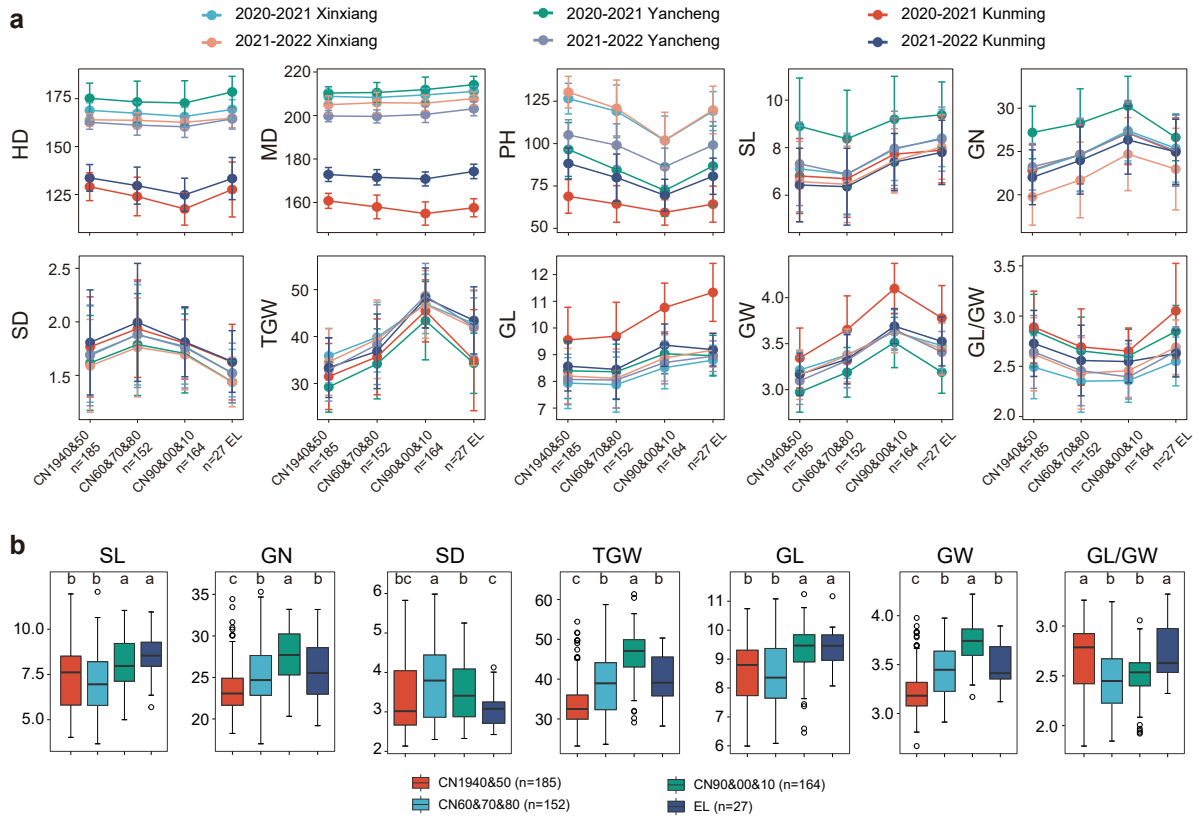


Extended Data Fig. 1 | Population diversity analysis of the 532 barley cultivars. Principal component analysis of the 532 barley cultivars analyzed in this study that are colored by different groupings. Gray dots at the background represent the 19,778 globally diversified Genebank accessions[29]. Percentages on the axes indicate variance explained by PC1 and PC2.

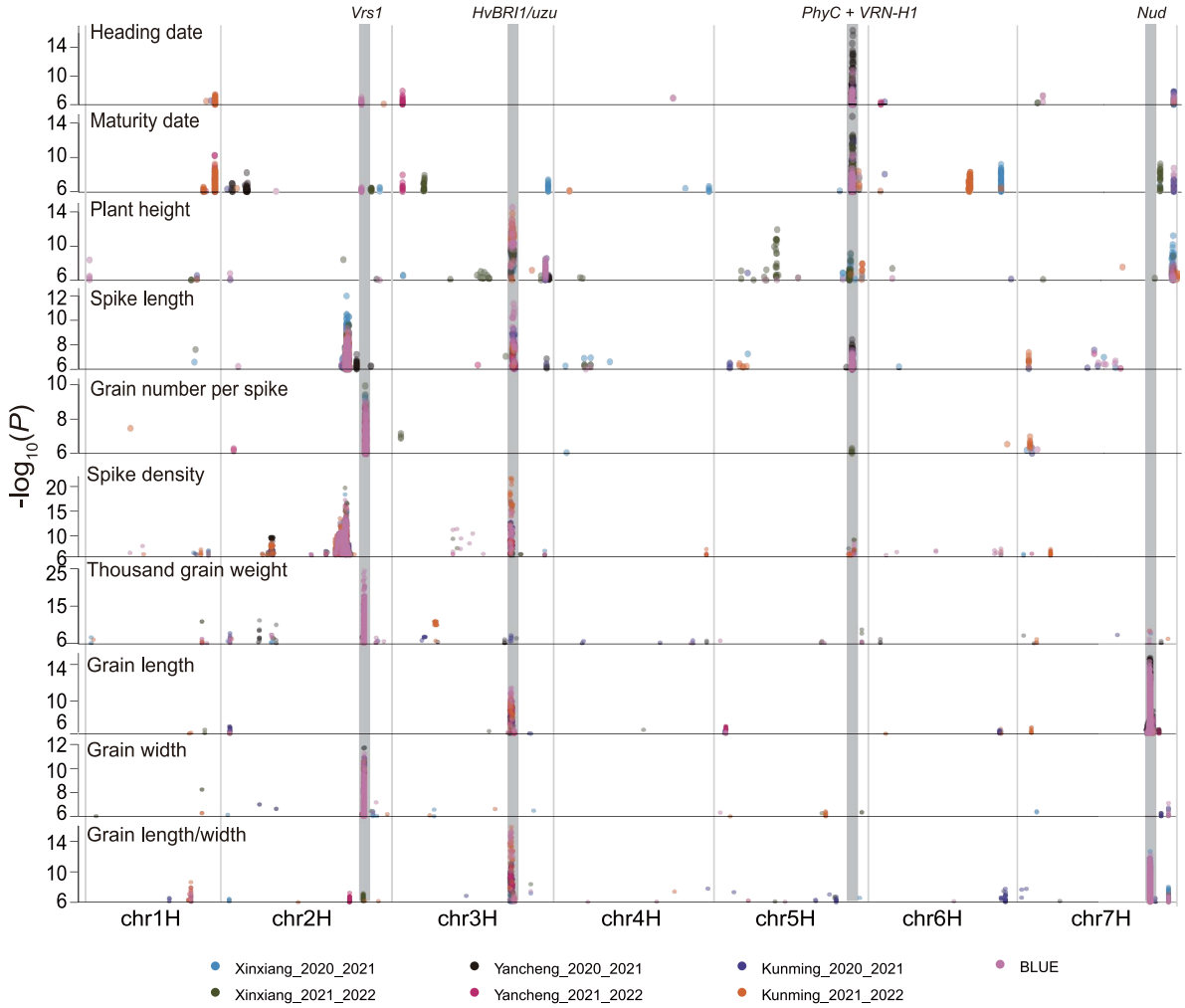


Extended Data Fig. 2 | See next page for caption.

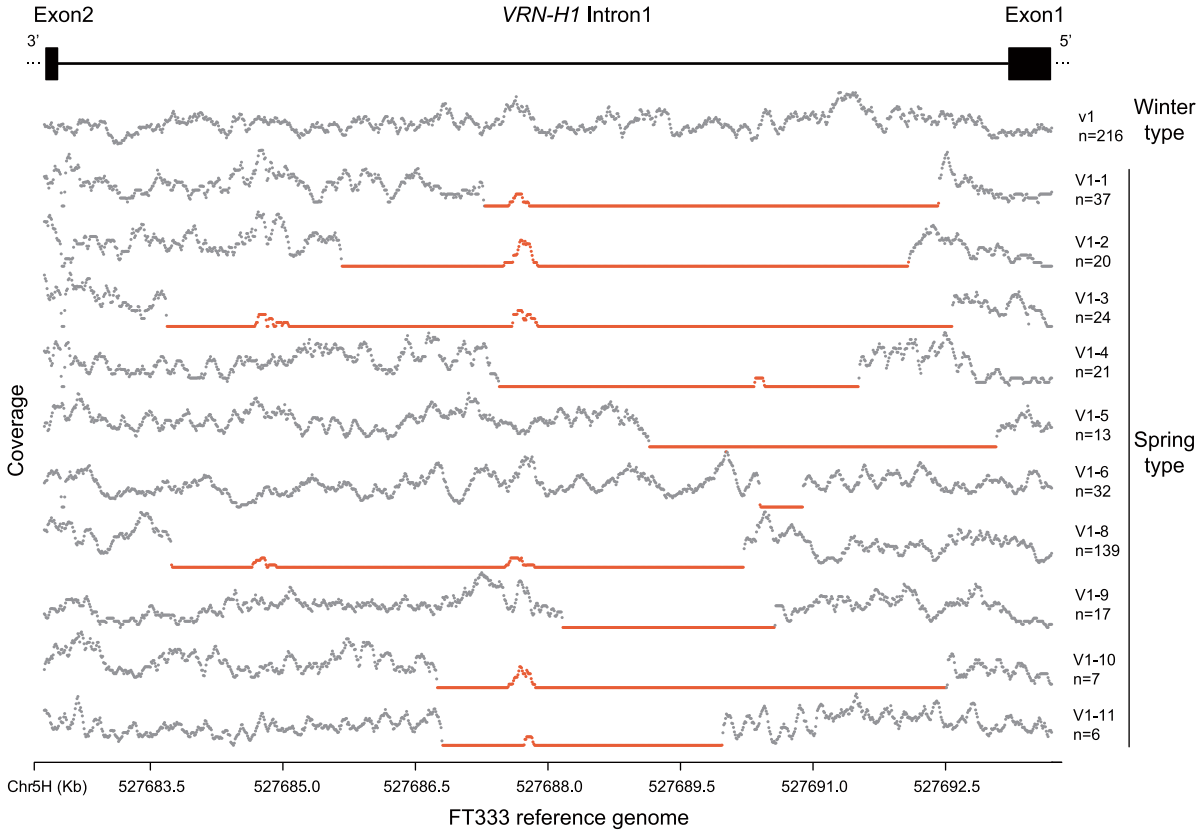
Extended Data Fig. 2 | Foundation lines in Chinese barley Breeding. **a**, A genomic-based germplasm network (GGNet)[48] generated based on 23,609,453 filtered SNPs among the 532 barley cultivars. 430 cultivars were identified involving in network with their germplasm identity-by-descent (gIBD) value, and five independent groups were identified, including group 3 which further partitioned into three subgroups, including Chinese historic cultivars enriched in group 3-1 and Qingke enriched in group 3-3. Each colored circle represents a cultivar, while its size indicates the summed gIBD values with all its related varieties. **b**, PCA showing the genetic distribution of the five GGNet groups within the 19,778 globally diversified Genebank accessions[29]. **c**, Ancestral haplotype groups (AHGs) on the seven chromosomes of the 430 barley varieties that were identified involving in genomic-based germplasm networks (GGNet). AHGs were inferred by IntroBlocker pipeline[50] using 1 Mb non-overlapping windows. The 20 most frequent AHGs are shown in various colors.



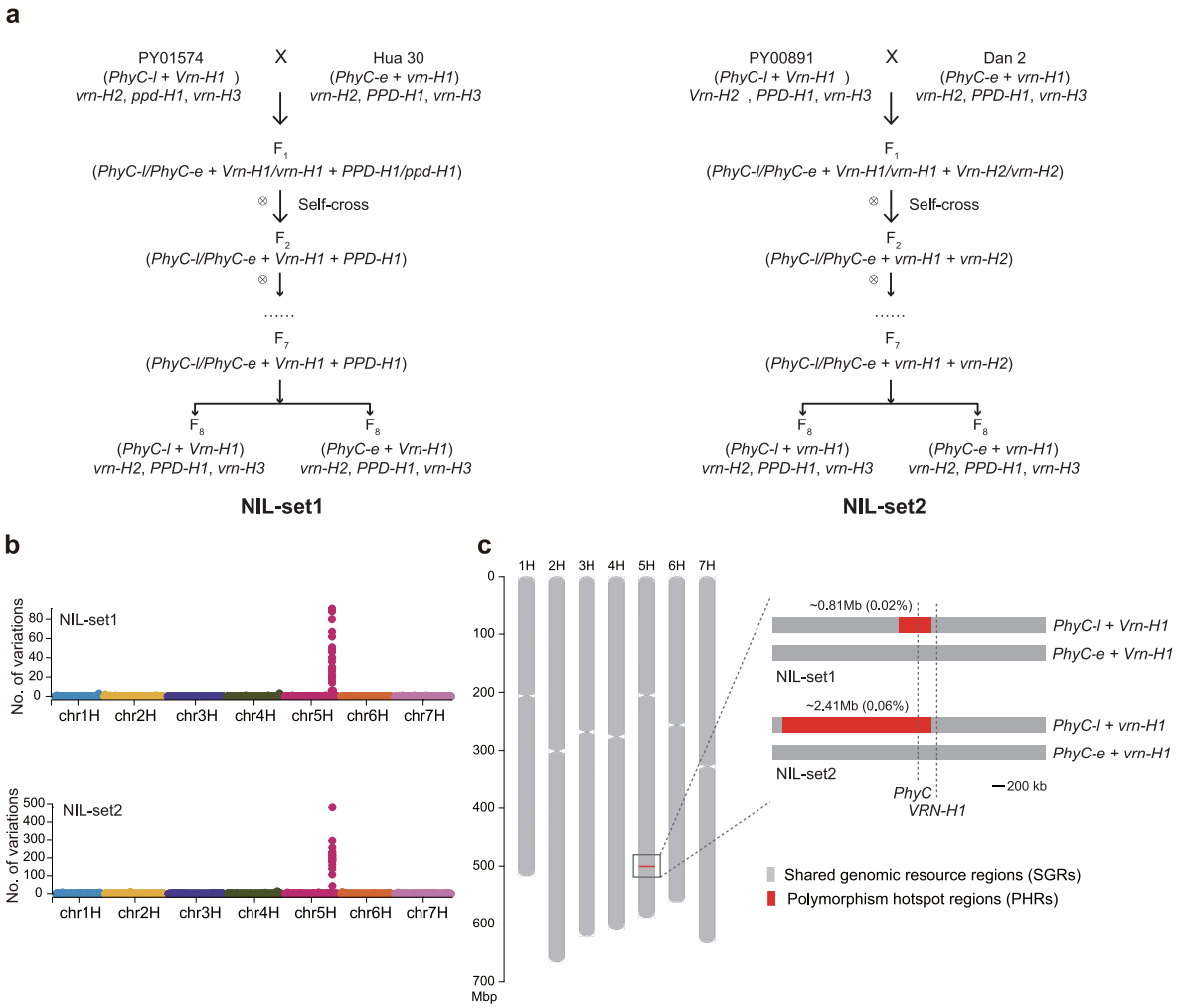
Extended Data Fig. 3 | Phenotypic changes of the 532 barley cultivars. **a**, The phenotypic variation of ten agronomic traits across three years and two locations. HD, heading date; MD, maturity date; PH, plant height; SL, spike length; GN, grain number on two rows per spike (two of six rows are counted in six-rowed barley); SD, spike density; TGW, thousand grain weight; GL, grain length; GW, grain width; GL/GW, ratio of grain length/grain weight. The cultivars are grouped according to breeding periods, and the 27 exotic lines are taken as outer group. The colored circles represent the mean value, while error bars represent standard deviation (mean ± SD). **b**, The best linear unbiased estimation (BLUE) values of seven traits across multiple trials. Box plots show the 25%–75% interval of raw value in the box, with central lines indicate the median, and whiskers extending to the minimum and maximum values within 1.5× of the interquartile range; outliers beyond this range are shown as individual circles. Different letters indicate significant differences at $p \leq 0.05$, determined by one-way ANOVA followed by Fisher's LSD test.



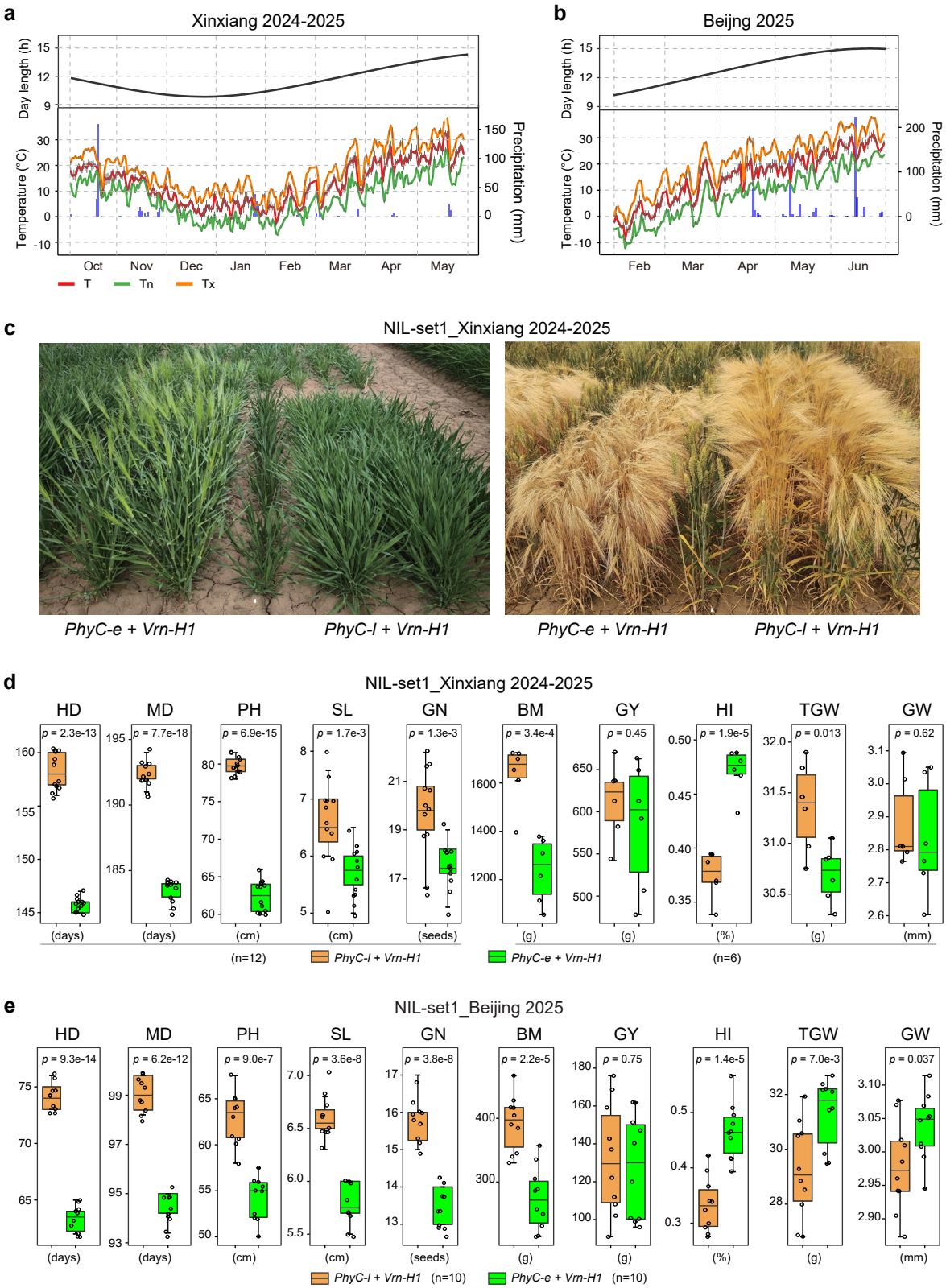
Extended Data Fig. 4 | GWAS for ten agronomic traits from seven datasets. The labels indicate each field trial as 'location_year' and the best linear unbiased estimate (BLUE) across multiple trials. The known loci with key regulatory genes underneath for spike (*Vrs1*) and grain characters (*uzu*/*HvBRI1*, and *NUD*) are marked.



Extended Data Fig. 5 | Schematic representation of the *VRN-H1* haplotypes based on the deletion pattern in its intron 1. The reference sequence was retrieved from a pangenome accession 'FT333'[30], which is a winter-type wild barley having the intact intron 1 of *VRN-H1*. Nomenclature of the spring-type haplotypes *V1-1* to *V1-11* are following the variants reported by Hemming et al.[34]. Orange dots indicate deletions present in each spring-type *Vrn-H1* haplotype.

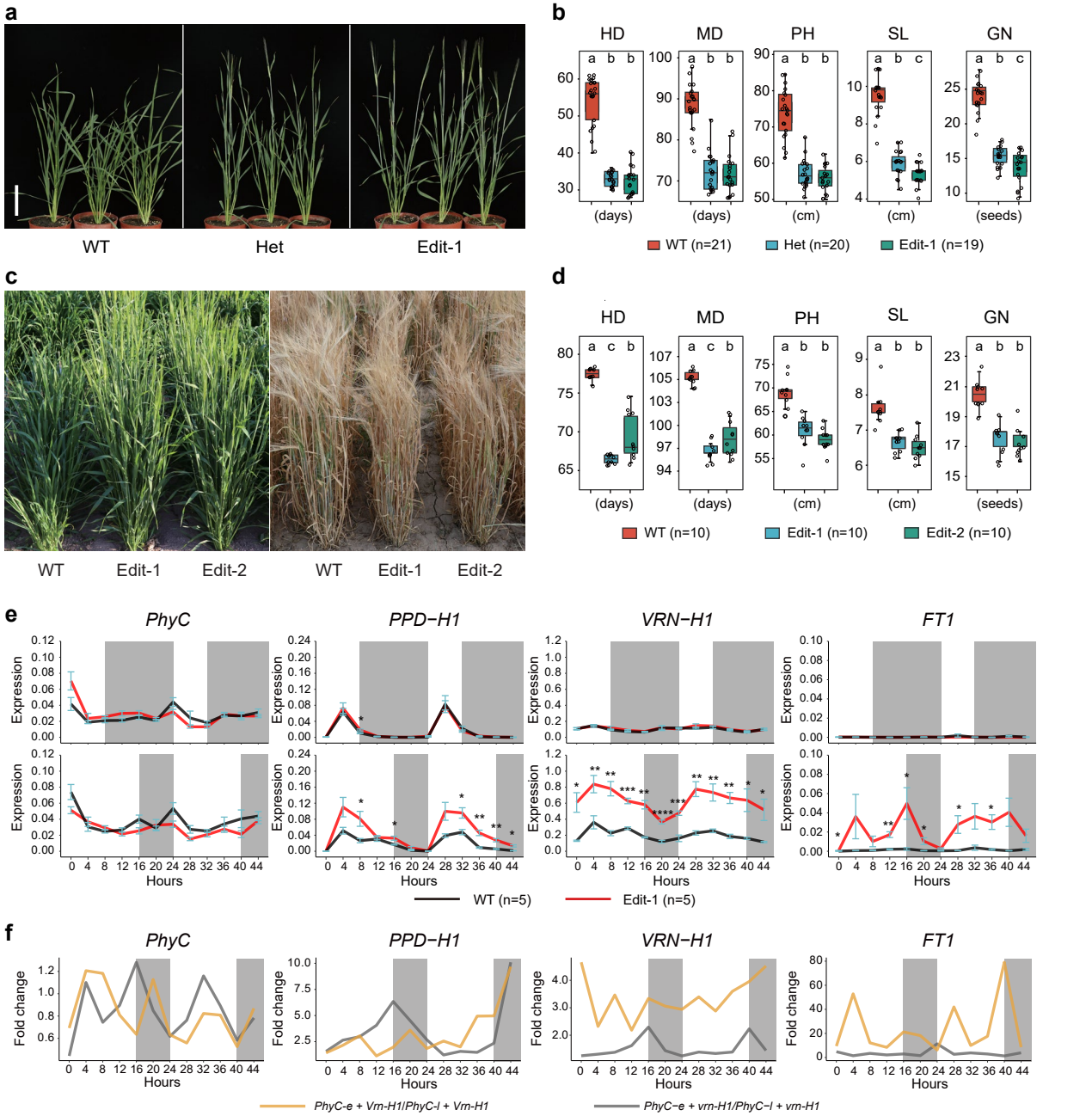


Extended Data Fig. 6 | Generation of near isogenic lines (NILs) that segregate at *PhyC* on distinct background of *VRN-H1* haplotype, respectively. **a**, Working pipeline for generating the two sets of NILs. **b**, Homogeneity at the genomic background was identified by whole-genome sequencing. **c**, Graphical representation of NILs lines. PHR, polymorphism hotspot regions; SGR, Shared Genomic resource Regions.

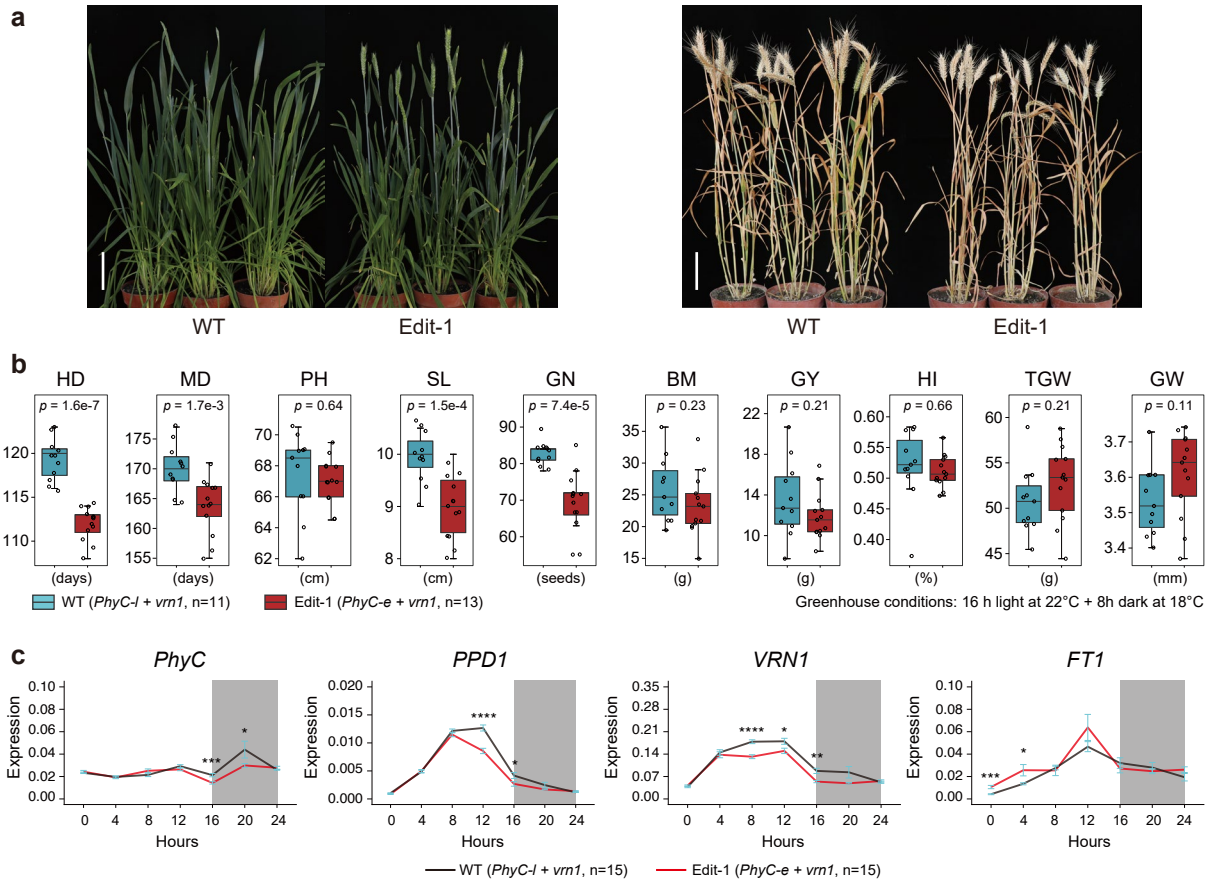


Extended Data Fig. 7 | See next page for caption.

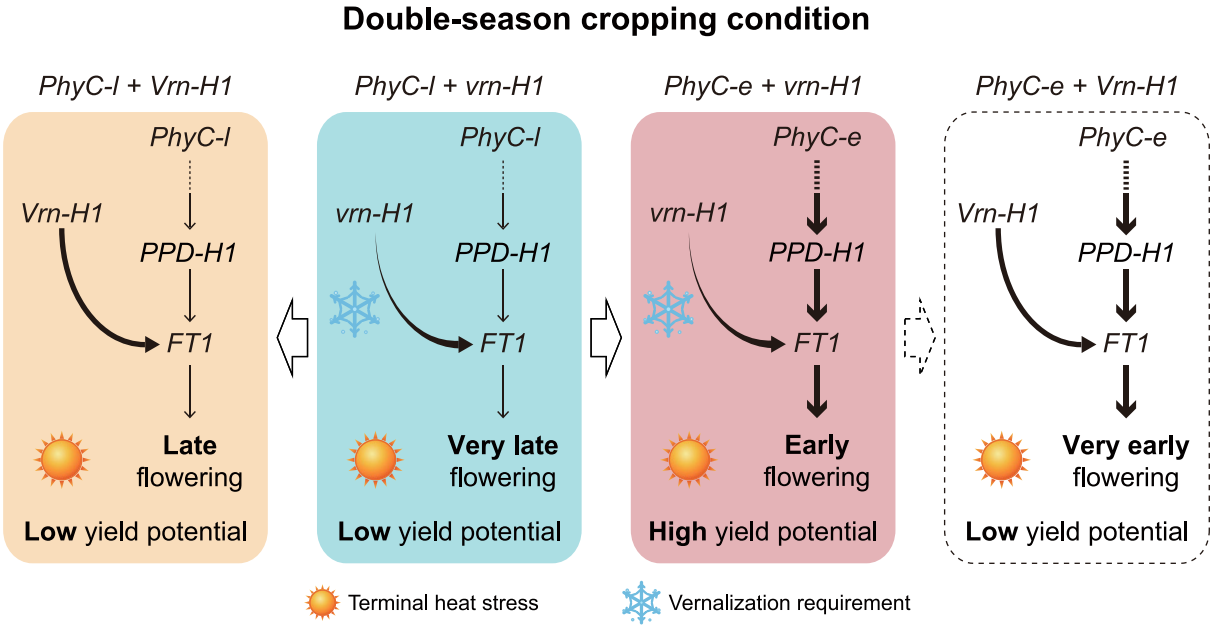
Extended Data Fig. 7 | Agronomical performance of NIL-set1 which exhibits the *PhyC* genotypic segregation on the background of spring-type *VRN-H1*. **a-b**, Climatic parameters in the autumn-sown trial in Xinxiang (**a**) and the early-spring sown trial in Beijing (**b**), respectively. The average day length (bold curve), daily temperature and precipitation (blue bar) were retrieved from https://rp5.ru/. T, average daily temperature (red); Tn, the minimum daily temperature (green); Tx, the maximum daily temperature (orange). **c**, Phenotype at the heading (left) and maturing (right) stage in Xinxiang. **d-e**, Statistics for 10 agronomic traits in Xinxiang (**d**) and Beijing (**e**), respectively. HD, heading date; MD, maturity date; PH, plant height; SL, spike length; GN, Grain number per spike; BM, biomass; GY, grain yield; HI, harvest index; TGW, thousand grain weight; GW, grain width. In (**d**), each genotype contained 12 replicates planted in rows, while row harvest each served as a measurement for HD, MD, PH, SL and GN; for the latter five traits (BM, GY, HI, TGW and GW), two-row harvest each served as a measurement, representing as 6 replicates. In (**e**), each genotype contained 10 replicates planted in rows, while row harvest each served as a measurement. Box plots show the 25%–75% interval of raw value in the box, with central lines indicate the median, and whiskers extending to the minimum and maximum values within 1.5× of the interquartile range. Each individual value (n) represents a biologically independent replicate. Statistical significance was estimated using two-tailed *t*-test.



Extended Data Fig. 8 | Phenotypes of base-edited barley *PhyC-e* plants under long-day greenhouse and field conditions. a, Phenotype at the heading stage of heterozygous and homozygous *PhyC-e* plants in comparing with the wild-type plants under greenhouse conditions. Scale bar, 10 cm. **b**, Statistics for five agronomic traits in the greenhouse. **c**, Phenotype of two homozygous *PhyC-e* edited lines in comparing with the wild-type plants at the heading and maturing stages under field conditions. **d**, Statistics for five agronomic traits under field conditions. In **b** and **d**, box plots show the 25%–75% interval of raw value in the box, with central lines indicate the median, and whiskers extending to the minimum and maximum values within 1.5× of the interquartile range. Each individual value (n) represents a biologically independent replicate. Different letters indicate significant differences at $p \le 0.05$, determined by one-way ANOVA followed by Fisher's LSD test. **e**, Transcriptional pattern of flowering regulation genes under short-day and long-day conditions. Gray shading indicates the nighttime duration. Statistical significance was determined using a two-tailed *t*-test (*$p \le 0.05$; **$p \le 0.01$; ***$p \le 0.001$; ****$p \le 0.0001$; ns, not significant; ns is not shown in the figures). Data are presented as mean ± standard error (SE). **f**, Fold change of flowering related genes transcription in *PhyC-e* versus *PhyC-l* on different *VRN-H1* alleles backgrounds.



Extended Data Fig. 9 | Phenotypes of base-edited wheat *PhyC-e* plants under long-day greenhouse conditions. a, Phenotypes of homozygous *PhyC-e* edited lines in comparing with wild-type plants at the heading and maturing stages. Scale bar, 10 cm. **b**, Statistical analysis of ten agronomic traits. Box plots show the 25%–75% interval of raw value in the box, with central lines indicate the median, and whiskers extending to the minimum and maximum values within 1.5× of the interquartile range. Each individual value (n) represents a biologically independent replicate. **c**, Transcriptional profiles of flowering regulatory genes under long-day conditions. Gray shading indicates nighttime duration. Data are presented as mean ± standard error (SE). Significance of difference was determined using a two-tailed *t*-test (*$p \le 0.05$; **$p \le 0.01$; ***$p \le 0.001$; ****$p \le 0.0001$; ns, not significant; ns is not shown in the figures).



Extended Data Fig. 10 | Schematic diagram illustrating the regulatory model of flowering time and the selection of the genetic modules in barley natural germplasm. The photoreceptor *PhyC* functions as an upstream flowering regulator in grass species, promoting the expression of the photoperiodic responser *PHOTOPERIODIC 1* (*PPD1*) and the flowering inducer *FT1* (*VERNALIZATION 3*)[21–23]. The ancient haplotype *PhyC-l*, in combination with the winter-type *vrn-H1* allele that requires vernalization, delays the transition from vegetative to reproductive growth, thereby preventing flowering (2nd panel, blue). In contrast, the spring-type *Vrn-H1* variant, which carries a truncation in the first intron of *VRN-H1* and eliminates the need of vernalization, enable flowering without cold exposure (1st panel, yellow). This allele in conjugation with *PhyC-l* is commonly adapted to spring-sown regimes in high-latitude or high-altitude regions. The East Asian-specific *PhyC*-e variant, which carries an F380S substitution at the *PhyC* locus and is consistently associated with winter-type *vrn-H1* allele, promotes early flowering and supports adequate biomass accumulation (3rd panel, pink). The *PhyC-e* + *vrn-H1* module allows barley to escape terminal heat stress, safeguard final yield, and fit to double-season cropping systems by leaving sufficient time for subsequent crops. This module has been widely selected in China's Yangtze River basin. Notably, the haplotype combination *PhyC-e* + *Vrn-H1* was not detected in barley natural germplasm (4th panel, dashed line). In this study, this novel module was generated either by base editing or by linkage breaking in the near-isogenic lines (NILs). It resulted in extremely early flowering and maturity, significantly reduced biomass, and undetected grain yield. This module holds potential for application in regions with extremely short growing seasons, such as those at very high latitudes or altitudes and at subtropical zones.

nature portfolio

Corresponding author(s): Ping Yang

Last updated by author(s): Sep 03,2026

Reporting Summary

Nature Portfolio wishes to improve the reproducibility of the work that we publish. This form provides structure for consistency and transparency in reporting. For further information on Nature Portfolio policies, see our Editorial Policies and the Editorial Policy Checklist.

Statistics

For all statistical analyses, confirm that the following items are present in the figure legend, table legend, main text, or Methods section.

n/a	Confirmed	
☐	☒	The exact sample size (*n*) for each experimental group/condition, given as a discrete number and unit of measurement
☐	☒	A statement on whether measurements were taken from distinct samples or whether the same sample was measured repeatedly
☐	☒	The statistical test(s) used AND whether they are one- or two-sided *Only common tests should be described solely by name; describe more complex techniques in the Methods section.*
☒	☐	A description of all covariates tested
☒	☐	A description of any assumptions or corrections, such as tests of normality and adjustment for multiple comparisons
☐	☒	A full description of the statistical parameters including central tendency (e.g. means) or other basic estimates (e.g. regression coefficient) AND variation (e.g. standard deviation) or associated estimates of uncertainty (e.g. confidence intervals)
☐	☒	For null hypothesis testing, the test statistic (e.g. *F*, *t*, *r*) with confidence intervals, effect sizes, degrees of freedom and *P* value noted *Give P values as exact values whenever suitable.*
☒	☐	For Bayesian analysis, information on the choice of priors and Markov chain Monte Carlo settings
☒	☐	For hierarchical and complex designs, identification of the appropriate level for tests and full reporting of outcomes
☒	☐	Estimates of effect sizes (e.g. Cohen's *d*, Pearson's *r*), indicating how they were calculated

Our web collection on statistics for biologists contains articles on many of the points above.

Software and code

Policy information about availability of computer code

Data collection	DNBSEQ-T7 platform (PE150)
Data analysis	Software used: lme4 (version 1.1.37), Cutadapt (version 3.3), Minimap2 (version 2.20), SAMtools (version 1.9), NovoSort (version 3.06.05), BCFtools (version 1.9), PLINK (version 1.9), ADMIXTURE (version 1.3.0), CLUMPP (version 1.1.2), TreeBeST (version 1.9.2), VCFtools (version 0.1.16), Cytoscape (version 3.10.1), Beagle (version 5.4), Gemma (version 0.98.5), Sequencher (version 4.8), DNASP (version 6.12.03), PopART (version 1.7), PROVEAN (version 1.1.5), R (version 4.2.3), XP-CLR (version 1.1.2), GEVA (version 1) Custom code availability: The nucleotide diversity was estimated by custom Perl scripts (Zeng et al., 2018, Nat. Commun., https://doi.org/10.1038/s41467-018-07920-5) The Identity-By-Descent (gIBD) segments were analyzed using the ggComp pipeline with 1Mb windows (Yang et al., 2022, Plant Physiol., https://doi.org/10.1093/plphys/kiac029) Ancestral haplotype groups (AHG) were delineated through the IntroBlocker pipeline with 1 Mb windows (Wang et al., 2022, Nat. Commun., https://doi.org/10.1038/s41467-022-31581-0) Haplotype block analysis was conducted with custom Perl scripts (Available at: https://github.com/guoyu-meng/barley-haplotype-script)

For manuscripts utilizing custom algorithms or software that are central to the research but not yet described in published literature, software must be made available to editors and reviewers. We strongly encourage code deposition in a community repository (e.g. GitHub). See the Nature Portfolio guidelines for submitting code & software for further information.

Data

Policy information about availability of data

All manuscripts must include a data availability statement. This statement should provide the following information, where applicable:

- Accession codes, unique identifiers, or web links for publicly available datasets
- A description of any restrictions on data availability
- For clinical datasets or third party data, please ensure that the statement adheres to our policy

Sequence data for 510 accessions generated in this study have been deposited at the China National Center for Bioinformation (CNCB) under BioProject ID PRJCA049684. Sequence data for an additional 22 accessions were obtained from the National Center for Biotechnology Information (NCBI) under BioProject ID PRJNA417220. Accession codes for all individual accessions are listed in Supplementary Table 2. The NCBI non-redundant protein database (nr) version 4, was used for protein sequence annotation and is available at https://ftp.ncbi.nih.gov/blast/db/v4/.

Research involving human participants, their data, or biological material

Policy information about studies with human participants or human data. See also policy information about sex, gender (identity/presentation), and sexual orientation and race, ethnicity and racism.

Reporting on sex and gender	Not applicable.
Reporting on race, ethnicity, or other socially relevant groupings	Not applicable.
Population characteristics	Not applicable.
Recruitment	Not applicable.
Ethics oversight	Not applicable.

Note that full information on the approval of the study protocol must also be provided in the manuscript.

Field-specific reporting

Please select the one below that is the best fit for your research. If you are not sure, read the appropriate sections before making your selection.

☒ Life sciences ☐ Behavioural & social sciences ☐ Ecological, evolutionary & environmental sciences

For a reference copy of the document with all sections, see nature.com/documents/nr-reporting-summary-flat.pdf

Life sciences study design

All studies must disclose on these points even when the disclosure is negative.

Sample size	No statistical methods were used to predetermine sample size. The 532 barley cultivars were selected based on 'China Barley Variety Directory' to broadly represent cultivated barley diversity in China. Sample sizes for near-isogenic lines, base-edited lines and their corresponding parental lines in barley, wheat and rice were determined by the availability of the relevant genetic materials and the requirements of each experiment.
Data exclusions	No data were excluded.
Replication	The field trials included 532 cultivars tested in six location-year combinations. Each experiment employed a design with two to three replications for every cultivar. All attempts at replication were successful.
Randomization	For the field trials, genotypes were allocated using a randomized complete block design with two to three replicates per genotype at each location. Randomization was performed within each replicate to minimize potential effects of field spatial variation. Randomization of experimental groups was not applicable to the GWAS because the analysis was based on naturally occurring genetic variation among the cultivars.
Blinding	Phenotypic measurements were taken independently by different scientists, across locations, and without knowledge of the underlying identifier of each accession. Hence all phenotypic measurements were blinded.

Reporting for specific materials, systems and methods

We require information from authors about some types of materials, experimental systems and methods used in many studies. Here, indicate whether each material, system or method listed is relevant to your study. If you are not sure if a list item applies to your research, read the appropriate section before selecting a response.

Materials & experimental systems

n/a	Involved in the study
☒	☐ Antibodies
☒	☐ Eukaryotic cell lines
☒	☐ Palaeontology and archaeology
☒	☐ Animals and other organisms
☒	☐ Clinical data
☒	☐ Dual use research of concern
☐	☒ Plants

Methods

n/a	Involved in the study
☒	☐ ChIP-seq
☒	☐ Flow cytometry
☒	☐ MRI-based neuroimaging

Dual use research of concern

Policy information about dual use research of concern

Hazards

Could the accidental, deliberate or reckless misuse of agents or technologies generated in the work, or the application of information presented in the manuscript, pose a threat to:

No	Yes
☒	☐ Public health
☒	☐ National security
☒	☐ Crops and/or livestock
☒	☐ Ecosystems
☒	☐ Any other significant area

Experiments of concern

Does the work involve any of these experiments of concern:

No	Yes
☒	☐ Demonstrate how to render a vaccine ineffective
☒	☐ Confer resistance to therapeutically useful antibiotics or antiviral agents
☒	☐ Enhance the virulence of a pathogen or render a nonpathogen virulent
☒	☐ Increase transmissibility of a pathogen
☒	☐ Alter the host range of a pathogen
☒	☐ Enable evasion of diagnostic/detection modalities
☒	☐ Enable the weaponization of a biological agent or toxin
☒	☐ Any other potentially harmful combination of experiments and agents

Plants

Seed stocks	532 cultivars include 505 popularly grown Chinese varieties spanning 80 years of breeding (186 in 1940s-1950s, 155 in 1960s-1980s, and 164 since 1990s) as well as 27 exotic lines (EL) that originated mostly from Europe and North America.
Novel plant genotypes	We used base editing approach to generate based-edited lines in barley, wheat and rice.
Authentication	Cultivars were provided by National Crop Genebank of China (NCGC) and further validated following the description of national barley variety directories published (Luo et al., 1989, Agriculture Press; China barley variety directory (1950-1985); Zhang et al., 2018, China Agricultural Science and Technology; China barley variety directory (1986-2015)).